Sustainable Energy & Fuels

ROYAL SOCIETY OF CHEMISTRY

PAPER

Published on 06 August 2026

Cite this: DOI: 10.1039/d6se00355a

Biogas and power to methanol *via* electrified steam methane reforming: a techno-economic optimisation

Andrea Nava and Matteo C. Romano *

This work assesses a process for the conversion of biogas into methanol, leveraging electrified steam methane reforming (eSMR) technology sustained by renewable electricity. This approach enables the design of flexible and compact reactors while avoiding biogas combustion and the loss of valuable biogenic carbon. The chemical process was simulated under both design and part-load conditions, evaluating various operating points. These include the introduction of hydrogen to regulate syngas composition and the utilisation of a biogas-fuelled Internal Combustion Engine (ICE) to self-generate electricity during periods of low availability of renewable power. The chemical island was integrated with intermittent renewable energy sources, Battery Energy Storage Systems (BESS), gas and liquid storage units. The overall configuration was optimised through annual simulations with hourly resolution, aiming to maximise the Net Present Value (NPV). The analysis considered two European locations, multiple economic scenarios, and different degrees of system flexibility, while evaluating the impact of methanol selling price and project scale on economic performance. From a technical perspective, the electrification of the reformer increases carbon efficiency from 30–50% typical of a conventional Fired Tubular Reformer (FTR), up to 70%. Moreover, by integrating electrolytic hydrogen, carbon efficiencies approaching 100% can be achieved, albeit at the expense of higher capital costs and energy consumption. Indeed, assuming an electrolyser cost of 1000–1300 € kW^{-1}, increasing the total product yield becomes profitable only when the methanol selling price exceeds approximately 1000 € t^{-1}. Notably, the operational flexibility of the chemical island enables a reduction in the production cost of up to 24% compared to an inflexible plant. Finally, transitioning to centralised biogas hubs leverages economies of scale and reduced biogas costs, driving the specific methanol production cost down from 760–1009 € t^{-1} for small-scale distributed plants (2.1 MW_{LHV} input) to 529–663 € t^{-1} for large-scale operations (21 MW_{LHV} input).

Received 26th March 2026
Accepted 9th July 2026

DOI: 10.1039/d6se00355a

rsc.li/sustainable-energy

1 Introduction

The significance of biogas as an energy carrier in the pursuit of decarbonisation objectives is growing. Typically produced and consumed locally, it plays a crucial role in enhancing national energy security and offers a unique opportunity to expand energy access. As a widely distributed resource, it contributes to the development of rural and agricultural areas while facilitating waste management. Furthermore, when utilised efficiently, biogas substantially reduces greenhouse gas emissions. Considering global bioenergy production, biogas represents a minor fraction, making up only 3% of the total modern bioenergy supply, equivalent to approximately 1% of global natural gas demand.[1] However, interest in this sector is steadily growing, driven by the potential to achieve negative emissions and the strong appeal of biomethane as a "drop-in" substitute for natural gas. Global production of biogas and biomethane rose from approximately 300 PJ in 2000 to nearly 1800 PJ by the end of 2023 (on an LHV basis), corresponding to nearly 50 billion cubic metres of natural gas equivalent (bcme).[1] Europe is the region that has most significantly expanded biogas production and currently accounts for nearly half of the global supply. In this region, biomethane output has increased more than tenfold since 2011, reaching 52 TWh in 2023 across 1510 upgrading plants.[2] Nevertheless, a critical factor for biomethane facilities is proximity to the natural gas grid, as connection costs are largely determined by the distance between the plant and the injection point. To date, 80% of global biogas supply is combusted for power and heat generation or utilised in buildings for cooking. Consequently, it is crucial to evaluate alternative pathways for the efficient utilisation of biogas, where biogenic carbon can be retained in the final product to displace fossil carbon. In this context, the electrification of steam methane reforming (eSMR) is particularly suitable, as it enables enhanced syngas production, compact reactor designs, and

Politecnico di Milano, Department of Energy, Via Lambruschini 4, 20156 Milan, Italy. E-mail: matteo.romano@polimi.it

flexible operation by avoiding combustion and the associated equipment that limit the economic competitiveness of conventional Fired Tubular Reformers (FTRs) at small scale. This facilitates the development of reactors suitable for small-scale, distributed generation, capable of flexible part-load operation to match the intermittency of renewable energy sources.[3]

The concept of electrified reforming, initially proposed by Spagnolo *et al.*[4] and later applied to biogas by Camacho *et al.*,[5] demonstrates a rapid thermal response that makes it highly flexible and well-suited for integration with intermittent renewable energy sources. Recently, Wismann *et al.* and Topsoe developed the eREACT™ technology,[6–9] currently being tested at the Aarhus University biogas research facility pilot plant. This represents the first application of an eSMR fed with biogas (15–27 $Nm^3\ h^{-1}$) sourced from a small industrial-scale biogas production plant. Experimental campaigns highlight the system's design flexibility, enabling fast transient operations, high temperatures, and heating rates of up to 330 °C h^{-1}, with a projected efficiency of 99% at the megawatt scale.[10] Furthermore, advanced control systems can stabilise the oxygen-to-carbon and hydrogen-to-carbon ratios despite fluctuations in the CH_4/CO_2 inlet composition, ensuring a stoichiometric syngas suitable for methanol synthesis under industrial conditions (900–1050 °C, 6–10 barg).[11] Recent pilot-scale studies have demonstrated the ability to dynamically switch between CH_4-rich and CO_2-rich feedstocks within the same electrified unit. This feed flexibility leverages corresponding changes in net energy consumption to balance the electrical grid, compensating for renewable intermittency without sacrificing production throughput.[12] Adopting conductive structured catalysts can further intensify electrified reforming. These configurations significantly improve reactor compactness and operational adaptability by enhancing heat and mass transfer, mitigating flow maldistribution, and optimising pressure drops.[13–20]

Considering the advantages of this technology, this study investigates bio-e-methanol production *via* an eSMR reactor. Electrifying the reformer avoids feedstock combustion for process heat, thus preserving valuable biogenic carbon and enhancing methanol yields compared to conventional technologies.

A primary challenge when using biogas is its inherently high CO_2 content, which generates hydrogen-deficient syngas with a stoichiometric module (M) below the optimal target (slightly above 2).[21–23] Although the syngas composition could be regulated through CO_2 removal,[24] this approach involves the loss of biogenic carbon. Therefore, the addition of external hydrogen offers an effective strategy to maximise the overall carbon efficiency of the process.[25,26]

Although some studies have investigated methanol production from biogas *via* dry and steam methane reforming,[27–30] techno-economic assessments of the integrated process remain limited. Consequently, only a few studies are available in the literature, and none have explored the potential of electrified reforming.

For instance, Hernández and Martín[31] and Rinaldi *et al.*[24] reported that 26–32% of the inlet biogas is combusted to sustain the endothermic reactions, capping carbon efficiencies between 34% and 50%. Alternatively, Sheets and Shah required an external natural gas stream equivalent to 30% of the feedstock energy.[32] Furthermore, to adjust the syngas stoichiometry, these studies typically rely on CO_2 removal either upstream or downstream of the reformer,[24,31,33] which further decreases the overall carbon utilisation. The estimated methanol production costs vary drastically across these conventional configurations, ranging from 380 € t^{-1} (assuming free biogas) to over 2100 US$ t^{-1}, heavily depending on the underlying economic assumptions and specific biogas pricing.[24,31–33]

This study proposes a conversion pathway for the production of bio-e-methanol (Fig. 1). The process entails the following steps: (i) syngas generation *via* electrified reforming; (ii) methanol synthesis; and (iii) methanol purification. Furthermore, the integration of electrolytic hydrogen generation to regulate the syngas composition is evaluated. The plant is designed for flexible operation, as it is powered by intermittent renewable energy sources. Consequently, this work aims to address the existing literature gaps through:

- A comprehensive process analysis, including the study of plant behaviour at part load and at different operating points (*i.e.* with/without hydrogen addition).
- System-level integration, modelling the processes with intermittent renewable sources, Battery Energy Storage Systems (BESSs), gas and liquid storage units, and the possibility to exploit a biogas-fuelled Internal Combustion Engine (ICE) to sustain operations during periods with low availability of renewable power.

The overarching objective of this study is to evaluate the techno-economic performance of bio-e-methanol production and to assess the economic value of flexibility in different economic scenarios, geographical locations, plant scales, and methanol selling prices. Furthermore, a key novelty of this work lies in the optimisation strategy, which is designed to maximise the Net Present Value (NPV) rather than minimising the production cost. This approach is particularly suitable for processes where the final product yield varies according to the selling price and the overall capacity is constrained by a given feedstock availability.

2 Methods

The plant considered in this study processes 5000 kg h^{-1} (3900 $Nm^3\ h^{-1}$) of cleaned biogas (which has undergone pretreatment to remove H_2S, VOCs, and other sulphur-based compounds, to protect the steam methane reformer catalyst[34]), with a molar composition of 55% CH_4 and 45% CO_2, corresponding to a thermal input of 21.4 MW. Such a throughput is representative of large-scale biogas production. The detailed process flow diagram is illustrated in Fig. 2.

2.1 Process simulation

The aforementioned bio-e-methanol system was designed and simulated using Aspen Plus® with the Peng–Robinson thermodynamic model, which was re-calibrated to accurately

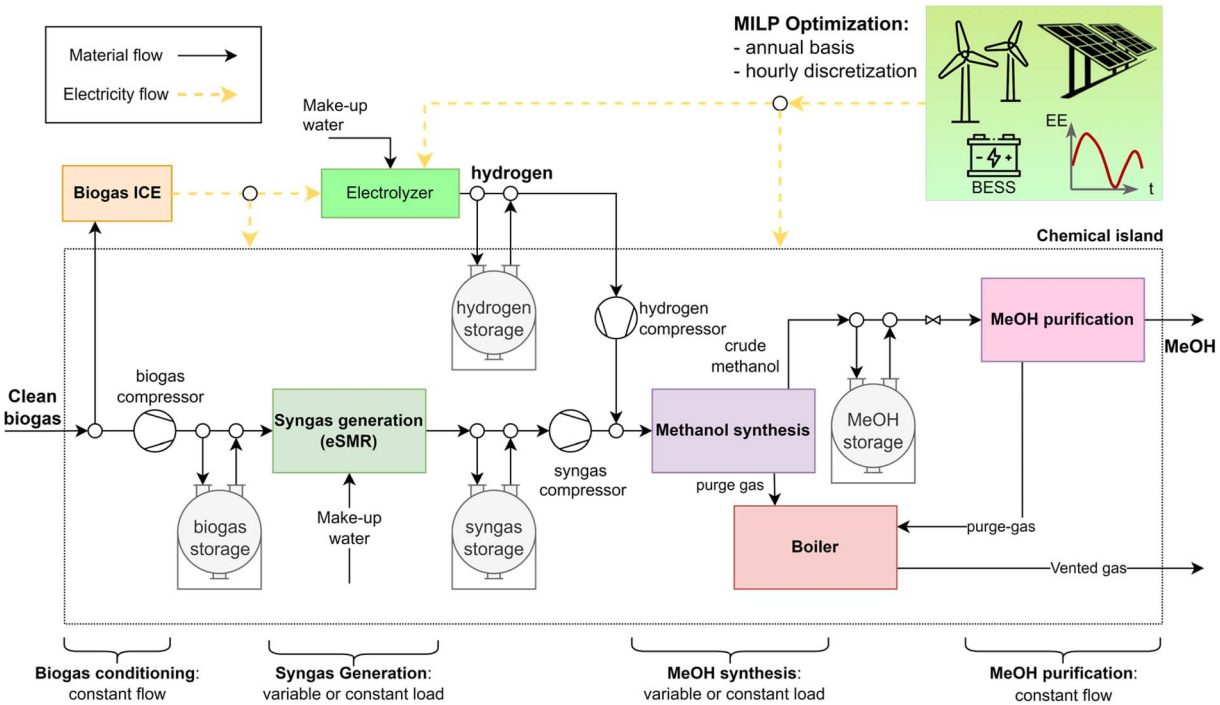

Fig. 1 Block diagram of the bio-e/MeOH process with power supply and storage systems.

predict the solubility of CO_2 in methanol, as described by Rinaldi *et al.*[24] The eSMR reactor is modelled at chemical equilibrium, with the thermal duty supplied *via* resistive heating (Joule effect). The electrical power is adjusted under partial load conditions to maintain an outlet temperature of 800 °C.

The methanol synthesis reactor is sized to have a Gas Hourly Space Velocity (GHSV) of 4000 $Nm^3\ h^{-1}\ kg_{cat}^{-1}$ at the reactor inlet under base load conditions and simulated as a one-dimensional homogeneous reactor, following the methodology of Rinaldi *et al.*[24] and employing the kinetic model proposed by Vanden Busche and Froment.[35] The reactor is cooled by boiling water at 30 bar (234 °C), resulting in a crude methanol outlet temperature of 240 °C.

The methanol loop recycle ratio (RR), defined as the ratio between the molar flow rate of recirculated gases (stream #31) and the fresh syngas feed (#23), is assumed to be 4.8 under base load conditions and is adjusted during partial load operation to maintain a constant molar flow rate at the reactor inlet, thereby ensuring a constant Gas Hourly Space Velocity (GHSV). However, when the chemical island operates in the electric neutral mode, the GHSV tends to drop due to the reduced syngas feed rate. Under these conditions, the recycle ratio is increased to mitigate this reduction, thereby preventing a critical drop in heat transfer coefficients and hot spots at partial load.

The main assumptions employed in the process simulations are listed in Table 1, while a detailed description of the chemical plant is provided in the SI. The methodology for modelling the plant's partial load behaviour, such as the procedures for calculating heat transfer coefficients in the heat exchangers, was adopted from the authors' previous work.[36] Consistently with this approach, heat transfer coefficients are calculated to be proportional to the mass flow rate raised to the power of n (with $n = 0.8$ for the shell & tube and $n = 0.67$ for plate heat exchangers).

2.2 Operating points and flexibility

The plant's inherent flexibility allows it to adapt to the intermittent availability of renewable energy by shifting between three primary operating modes:

- *Base load*: the entire biogas stream is processed to produce methanol without the addition of external hydrogen.
- *Enhanced MeOH*: hydrogen, either produced by the electrolyser or drawn from storage, is used to adjust the syngas composition to the optimal stoichiometric module ($M = 2.1$). This maximises biogenic carbon conversion and, consequently, methanol yield.
- *Electric neutral*: in the absence of renewable power, a - fraction of the biogas is diverted to the internal combustion engine (ICE) to generate the exact amount of electricity required by the chemical island.

To ensure flexible operation that maximises the use of intermittent renewable energy, the plant's design incorporates several storage units. A biogas tank allows the syngas production rate to be decoupled from the constant biogas supply; its rate can be ramped up during periods of high renewable availability by drawing from the tank or reduced by diverting biogas to storage when power is scarce. Downstream, syngas storage decouples the energy-intensive syngas generation section from the methanol synthesis loop. Similarly, hydrogen storage buffers the electrolyser's variable output, allowing hydrogen to be produced during power peaks and consumed

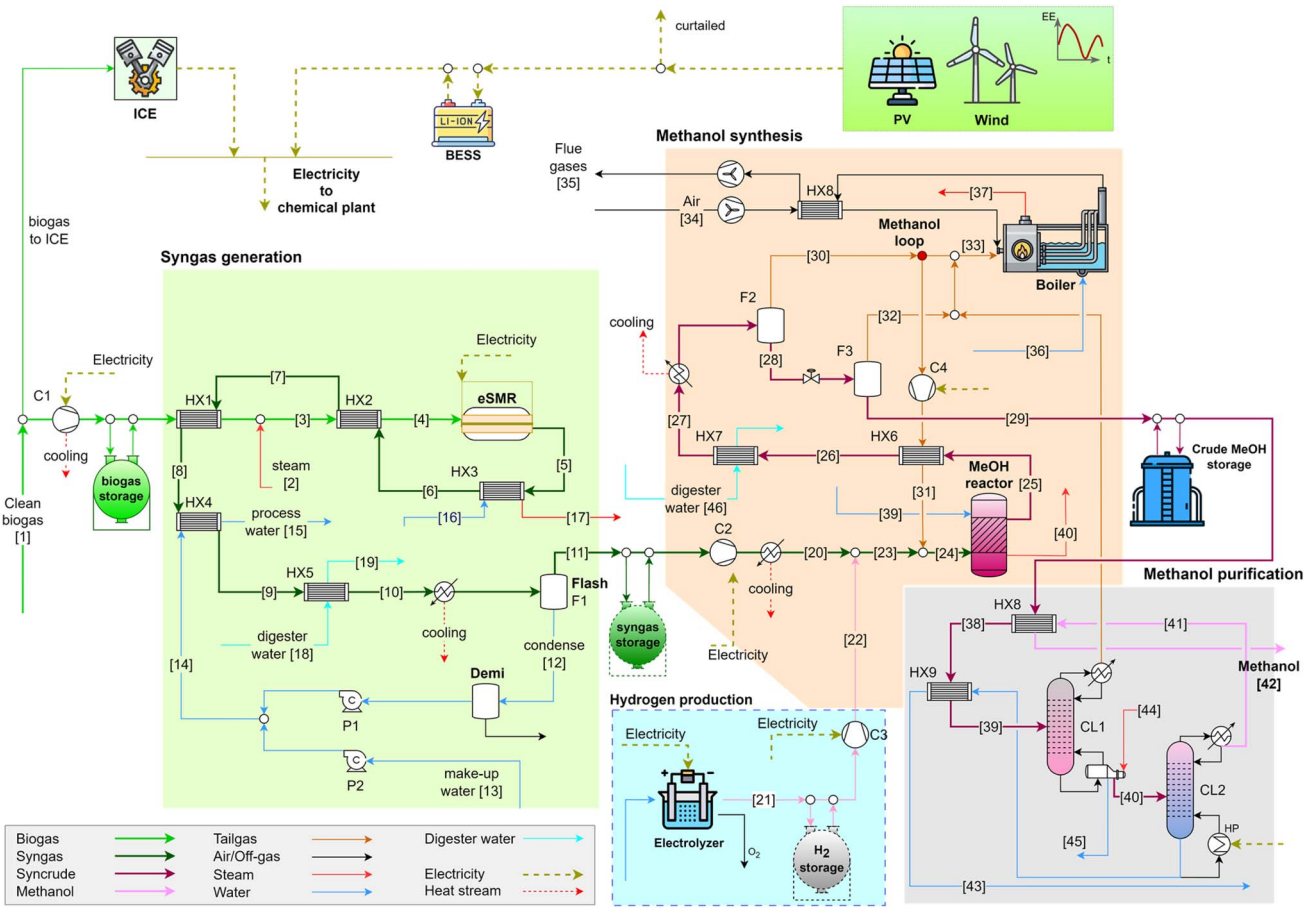

Fig. 2 Process flow diagram of the biogas to methanol plant based on electrified biogas reforming (eBGR). Syngas and hydrogen storage are only considered in the "enhanced flexibility" scenario.

steadily to adjust the syngas stoichiometric module. Finally, a crude methanol storage tank is used to buffer the variable output of the synthesis section, ensuring a constant feed to the distillation columns.

The electricity for the process is sourced from on-site photovoltaic (PV) panels and wind turbines. To manage short-term fluctuations and ensure a stable power supply, a lithium-ion Battery Energy Storage System (BESS) is also considered. The time-resolved generation profiles for the renewable sources are used as input data for the optimisation algorithm.

To quantify the economic benefit of operational flexibility, three distinct plant design scenarios with increasing degrees of freedom are compared:

- *Inflexible scenario*: the chemical island is constrained to operate at a constant, nominal load. The management of REN intermittency relies solely on the Battery Energy Storage System (BESS). The ICE (if installed) provides a firm baseload power from biogas combustion, thus reducing the installed capacity of renewables and batteries.
- *Flexible plant*: the chemical island can operate at partial load. The biogas storage enables the modulation of the feed rate to the syngas and synthesis sections, thus matching the plant's power consumption with REN power generation. Specifically, if an electrolyser is installed, the generated hydrogen is directly consumed by the synthesis unit without intermediate storage. The crude methanol storage decouples this operational flexibility from the purification unit, which is operated at steady state.
- *Enhanced flexibility*: intermediate storage for both syngas and hydrogen is included. This fully decouples the syngas generation, hydrogen production, and methanol synthesis units, providing the maximum degree of operational flexibility.

It should be noted that the inclusion of the electrolyser and its associated storage systems is a result of the techno-economic optimisation; therefore, the optimal plant configuration may not necessarily include these units. Furthermore, the hourly optimisation model neglects potential dynamic effects, assuming sufficient equipment flexibility to accommodate the required process load reductions.

2.3 Economic analysis and scenarios

The economic assumptions for the power generation units, ICE, electrolyser, and the chemical island's process equipment are presented in Table 3. The CAPEX of conventional components (*i.e.* distillation columns, heat exchangers, pumps, compressors, and flash drums) was estimated using the methodology reported by Turton.[37] This approach accounts for materials of

Table 1 Summary of the process design and Aspen Plus® simulation assumptions

Component	Parameter	Value	Unit
Biogas	Mass flow rate	5000	$kg\ h^{-1}$
	Volumetric flow rate	3900	$Nm^3\ h^{-1}$
	CO_2 content	45	$\%_{mol}$
	CH_4 content	55	$\%_{mol}$
Biogas ICE	Net electric efficiency	40	%
Electrified reformer (eSMR)	Calculation mode: chemical equilibrium		
	Outlet temperature	800	°C
	Inlet pressure	8	bar
	Pressure drop	1	bar
	Electric efficiency	99	%
Syngas flash (F1)	Adiabatic flash	30	°C
Methanol synthesis reactor: an RPLUG reactor with a constant thermal fluid temperature	Reactor pressure	93	bar
	Outlet temperature	240	°C
	Boiling water pressure	30	bar
	Boiling water temperature	234	°C
	Design gas hourly space velocity (GHSV) at the reactor inlet	4000	$Nm^3\ h^{-1}\ m_{cat}^{-3}$
	Tube length	6	m
	Tube diameter	4.2	cm
	Global heat transfer coefficient	280	$W\ m^{-2}\ K^{-1}$
	Catalyst pellet diameter	6	mm
	Density of spherical catalyst particles	1712	$kg\ m^{-3}$
	Bed void fraction	40	%
	Recycle ratio at base load	4.8	
	Recycle ratio at part load	Adjusted to keep the GHSV	
Flash separator (F2 & F3)	Adiabatic flash	40	°C
First distillation column (CL1)	Calculation mode: equilibrium, 7 stages plus a partial-vapor condenser and kettle reboiler		
	Methanol content in the vent (adjusted with the reflux ratio)	0.02	mol_{CH_3OH}/mol
	CO_2 content in the product (adjusted with the distillate to feed ratio)	0.0001	mol_{CO_2}/mol
Second distillation column (CL2)	Calculation mode: equilibrium, 14 stages plus a total condenser and kettle reboiler		
	Methanol purity (adjusted with the reflux ratio)	0.99	mol_{CH_3OH}/mol
	Purity of bottom water	0.99	mol_{H_2O}/mol
Pumps	Hydraulic efficiency	70	%
	Mechanical–electrical efficiency	94	%
Compressors	Biogas compressor (Compr) with coolers to have maximum outlet temperature	120	°C
	Syngas/hydrogen compressor (MCompr) with 3 stages and intercooler outlet temperatures (the last stage is adiabatic)	35	°C
	Isentropic efficiency	70	%
	Mechanical–electrical efficiency	92	%
Heat exchangers	Gas side pressure drop	2	% of p_{in}
	Liquid side pressure drop	5	bar
	Economiser water subcooling ΔT	14	°C
Boiler	Molar fraction of O_2 in flue gases	2	$\%_{mol}$
Heat transfer coefficients	Low-pressure gas	50	$W\ m^{-2}\ K^{-1}$
	Compressed gas	500	$W\ m^{-2}\ K^{-1}$
	Biogas/syngas in the pre-heater	120[a]	$W\ m^{-2}\ K^{-1}$
	Syngas with condensing water	2500[a]	$W\ m^{-2}\ K^{-1}$
	Water (liquid)	10 000	$W\ m^{-2}\ K^{-1}$
	Water (evaporation)	20 000	$W\ m^{-2}\ K^{-1}$

[a] Values obtained with a heat exchanger simulated using Aspen EDR (simulation mode) with inputs of streams from Aspen Plus.

construction, pressure ratings, direct and indirect project expenses, contingency, and contractor fees.[36,37] The cost of the methanol synthesis reactor was estimated using the methodology from Poluzzi *et al.*[25]

For the novel eSMR unit, the cost was estimated using the model from the authors' previous work,[36] which quantifies the required materials (*i.e.*, internal conductive structure, catalyst, electrical elements, refractory material and outer steel shell). The total installed cost, which includes labour, installation, indirect costs, and owner's costs and contingencies, was then determined using the methodology reported by Riva *et al.*[38] All capital costs were escalated to €2023 values using the Chemical Engineering Plant Cost Index (CEPCI).[39] Further details on the economic analysis are provided in the SI.

Given that the capital costs of PV, on- and off-shore wind, BESSs, and electrolysers are the primary drivers of the total annual cost,[36] three distinct economic scenarios were defined to assess their impact: (i) a short-term scenario, reflecting current technology costs;[40] (ii) a long-term scenario, which adopts cost projections for 2050 sourced from the NREL Annual Technology Baseline (ATB)[41] for the cost of PV, on-shore and off-shore wind and BESSs and assuming projections for electrolyser CAPEX based on the estimates from the U.S. Department of Energy (DOE), McKinsey & Company and the Hydrogen Council, which project 2050 electrolyser cost to remain in the range of 900–1200 \$ kW^{-1};[42,43] (iii) a long-term visionary scenario, which adopts optimistic cost targets found in technology-forward studies, such as those published by IRENA and LUT,[44,45] assuming radical learning-curve advancements for both PV and electrolyser technologies, projecting 2050 electrolyser CAPEX to fall as low as 100–400 € kW^{-1}.

2.4 MILP optimisation

The techno-economic optimisation of the entire integrated system was modelled using a mixed-integer linear programming (MILP) framework. The model was developed and implemented using GAMS and is designed to minimise the total annual cost based on three main categories of inputs:

- Hourly time-series data for renewable electricity generation (PV and wind).[46]
- Key economic assumptions (as listed in Table 3).
- A set of mathematical correlations describing the chemical island's performance.

Mathematical correlations of the chemical plant were derived from Aspen Plus® simulations conducted at various operating points and partial load. They define the relationships between the gas/liquid flow rates feeding each plant section and their corresponding electrical/thermal loads, production ratios, steam consumption/production and auxiliary demands, such as process and cooling water. The MILP framework employs binary variables and the "big-M" method to handle key discrete decisions. These are used for both investment decisions (*i.e.*, whether to install the ICE and the hydrogen production section) and operational decisions (*i.e.*, the switch on/off of these components in each time step). For instance, the activation of the electrolyser section triggers a change in the methanol synthesis equations within the model, reflecting the adjusted syngas composition and the subsequent increase in methanol yield.

The model is computed over one year of operation with hourly resolution. The energy balances connecting power generation (renewable sources with a BESS and ICE) and consumption (chemical plant and hydrogen production) are modelled based on the methodology described in ref. 36. This methodology also includes the equations governing the hourly state-of-charge (SoC) of the BESS and material storage tanks.

The algorithm's objective function is to minimise the total annual cost, which is solved using the CPLEX solver.

Objective function:

$$\text{Min (TAC)} = \text{CAPEX}\cdot\text{CRF} + f\text{OPEX} + v\text{OPEX} - \text{Revenues} \quad (1)$$

The optimisation yields both the optimal plant design and its year-long operating strategy. The key design variables determined by the model include the capacities of the renewable power plants and BESS, the maximum throughput of the chemical island sections and the electrolyser, and the size of all material storage tanks. Given that the optimal solution is highly dependent on the methanol selling price, a sensitivity analysis was performed on this key parameter. The detailed mathematical formulation of the model, including all governing equations and constraints, is provided in the SI.

2.5 Emissions

The embodied emissions associated with the renewable technologies used to power the system are presented in Table 2. This study considers both a low-emission and a high-emission scenario, which are representative of the emission ranges identified in the literature.[47–50] Furthermore, methane slip from the biogas production and storage chain is accounted for. Fugitive emissions can vary widely depending on the plant's technology, its operational management, and the quantification methodologies employed.[51] For instance, Hurtig *et al.* reported that methane losses from most biogas plants range from 0.5% to 6% of the methane produced.[52] In this work, a methane loss in the range of 0.5% to 2% (2.7 to 10.8 g_{CO_2}/MJ_{biogas}) of the total biogas produced is assumed. This range was selected to evaluate the sensitivity of the system's overall carbon footprint to fugitive emissions, acknowledging that these losses are highly variable and constitute a critical parameter affecting the final environmental performance.

Table 2 GWP potential of REN-BESS and methane slip

		Low	High	Ref.
PV	$kg_{CO_2,eq}/kW_{el}$	420	1400	47 and 48
Wind	$kg_{CO_2,eq}/kW_{el}$	380	650	49
BESS	$kg_{CO_2,eq}/kWh_{el}$	89	169	50
Methane slip	g_{CO_2}/MJ_{biogas}	2.70	10.80	52

Table 3 Economic assumptions for REN sources, storages and chemical islands in different economic scenarios

	Short-term	Long-term	Long-term visionary	units	Ref.
PV (fixed-tilt)					40, 45 and 53
Inv. cost (North Italy)	800	680	306	€ kW^{-1}	
Inv. cost (Denmark)	1148	680	306	€ kW^{-1}	
Fixed O&M	15	12	6	€ kW^{-1} $year^{-1}$	
Wind (on-shore)					40, 45 and 53
Inv. cost	1500	1210	1000	€ kW^{-1}	
Fixed O&M	45	36	20	€ kW^{-1} $year^{-1}$	
Wind (off-shore)					40, 45 and 53
Inv. cost (Denmark)	2772	2600	2449	€ kW^{-1}	
Fixed O&M	101	80	80	€ kW^{-1} $year^{-1}$	
BESS (lithium-ion)					40, 53 and 54
charge efficiency	95%	95%	95%	—	
Discharge efficiency	95%	95%	95%	—	
Energy/power ratio	4	4	4	kWh kW^{-1}	
Inv. cost	259	124	124	€ kWh^{-1}	
Fixed O&M	6.5	3.1	2.5	€ kWh^{-1} $year^{-1}$	
Variable O&M	0.09	0.04	0.04	€ MWh^{-1}	
Electrolyser					42–45
EE to H_2 efficiency (LHV)	58.5%	68.0%	68.0%	—	
Inv. cost	1300	1100	363	€ kW^{-1}	
Fixed O&M	26	22.0	12.7	€ kW^{-1} $year^{-1}$	
Variable O&M	13.3	13.3	1.0	€ MWh^{-1}	
Biogas ICE					55
Inv. cost	500			€ kW_{el}^{-1}	
Fixed O&M	100			€ kW^{-1} $year^{-1}$	
Variable O&M	10			€ MWh^{-1}	
H_2storage					56
Inv. cost	10			€ kWh^{-1}	
Fixed O&M	4% CAPEX			€ kWh^{-1} $year^{-1}$	
Bio-syngas storage					57
Inv. cost	62.3 [€ m^{-3}] × V [m^3] + 66 223 [€]			€ m^{-3}	
Fixed O&M	4% CAPEX				
Storage charge/discharge efficiency	100%				
Chemical island					24, 25, 36 and 37
eSMR reactor[a]	104 [€ Nm^{-3} h^{-1}] × V [Nm^3 h^{-1}] + 7492 [€]				
Cooling water	1.57×10^{-5}			€ kg^{-1}	
Process water	1.71×10^{-3}			€ kg^{-1}	
eSMR catalyst	50			€ kg^{-1}	
Methanol synthesis catalyst	11.8			€ kg^{-1}	
Catalyst lifetime	4			years	
Fixed O&M	4% Capex				
Other process equipment	See SI material				
Biogas	34–54			€ MWh^{-1}	
Financial					
Taxation rate	0 ÷ 30%			%	
Discount rate	8.78%			%	
Plant lifetime	25			years	

[a] eSMR reactor cost function considers the inlet volumetric flow of wet biogas.

2.6 KPIs

To assess and compare the techno-economic and environmental performance of the different scenarios analysed, the following Key Performance Indicators (KPIs) were defined.

2.6.1 Process. The single-pass yield (eqn (2)) quantifies the production of methanol in the synthesis reactor relative to the amount of CO and CO_2 in the reactor feed. The overall yield (eqn (3)) considers the amount of CO and CO_2 in the syngas feeding the synthesis section as the input and the methanol exiting the synthesis section.

$$Y_{SP} = \frac{\dot{N}_{MeOH,out} - \dot{N}_{MeOH,in}}{\dot{N}_{CO,in} + \dot{N}_{CO_2,in}} = \frac{\dot{N}_{MeOH,\#25} - \dot{N}_{MeOH,\#24}}{\dot{N}_{CO,\#24} + \dot{N}_{CO_2,\#24}} \quad (2)$$

$$Y_{GL} = \frac{\dot{N}_{MeOH}}{\dot{N}_{CO,syngas} + \dot{N}_{CO_2,syngas}} = \frac{\dot{N}_{MeOH,\#29}}{\dot{N}_{CO,\#23} + \dot{N}_{CO_2,\#23}} \quad (3)$$

Alternatively, the single-pass and overall yields can be expressed based on hydrogen as the reference reactant, noting

that two moles of hydrogen are required to produce one mole of methanol (eqn (4) and (5)). This is relevant when syngas with M lower than 2 is fed to the methanol synthesis section and methanol yield is constrained by the availability of hydrogen.

$$Y_{SP,H_2} = \frac{\dot{N}_{MeOH,out} - \dot{N}_{MeOH,in}}{\dot{N}_{H_2,in}/2} = \frac{\dot{N}_{MeOH,\#25} - \dot{N}_{MeOH,\#24}}{\dot{N}_{H_2,\#24}/2} \quad (4)$$

$$Y_{GL,H_2} = \frac{\dot{N}_{MeOH}}{\left(\dot{N}_{H_2,syngas} + \dot{N}_{H_2,ext}\right)/2} = \frac{\dot{N}_{MeOH,\#29}}{\dot{N}_{H_2,\#23}/2} \quad (5)$$

The carbon efficiency represents the amount of biogenic carbon preserved in the produced methanol, as defined in eqn (6).

$$\eta_C = \frac{\dot{N}_{C,MeOH,prod}}{\dot{N}_{C,biogas}} = \frac{\dot{N}_{C,\#42}}{\dot{N}_{C,\#1}} \quad (6)$$

The methanol production energy ratio is defined in eqn (7) and quantifies the energy of the produced methanol (on an LHV basis) relative to the energy contained in the biogas feed.

$$\text{MPER(Methanol production energy ratio)} = \frac{\dot{m}_{MeOH} \cdot LHV_{MeOH}}{\dot{m}_{BG} \cdot LHV_{BG}} \left[\frac{kW_{MeOH}}{kW_{biogas}}\right] \quad (7)$$

The methanol production efficiency considers both the energy content of the biogas and the electricity consumed by the system (eqn (8)).

$$\eta_{MeOH} = \frac{\dot{m}_{MeOH} \cdot LHV_{MeOH}}{\dot{m}_{BG} \cdot LHV_{BG} + P_{el}} \left[\frac{kW_{MeOH}}{kW_{input}}\right] \quad (8)$$

The specific CO_2 emissions ($E_{CO_2,emit}$) quantify the amount of carbon dioxide emitted relative to the produced methanol (eqn (9)).

$$E_{CO_2,emit} = \frac{\dot{m}_{CO_2,emit}}{\dot{m}_{MeOH}} \left[\frac{kg_{CO_2}}{kg_{MeOH}}\right] \quad (9)$$

The specific electricity consumption (E_{el}) quantifies the net electricity consumed by the system per unit of methanol produced (eqn (10)).

$$E_{el} = \frac{P_{el}}{\dot{m}_{MeOH}} \left[\frac{kWh_{el}}{kg_{MeOH}}\right] \quad (10)$$

The battery equivalent cycle number (BCY) is defined as the ratio of the total annual renewable energy charged into the battery to its nominal capacity (eqn (11)). This parameter provides an estimate of the equivalent charge/discharge cycles the battery undergoes during the year.

$$BCY = \frac{\sum_{t=1}^{8760} EE_{to\ BESS}(t) \cdot \Delta t}{SOC_{max}} \left[\frac{kWh}{kWh}\right] \quad (11)$$

The capacity of the biogas, syngas, crude methanol, and hydrogen storage units is expressed in storage hours (STH). This metric is calculated as the ratio of the total tank volume to the maximum volumetric flow rate of the corresponding stream (eqn (12)). Therefore, it represents the time required to completely fill or empty the tank at the maximum flow rate.

$$STH = \frac{BG_{stor,max}}{\dot{V}_{bg1}} [h] \quad (12)$$

2.6.2 Economics. The methanol production cost represents the total annualised cost of production (accounting for both CAPEX and OPEX) relative to the amount of methanol produced annually (eqn (13)). The capital recovery factor (CRF) is equal to 10% and is used to annualise the CAPEX, assuming a discount rate r of 8.78% and a plant lifetime of 25 years (eqn (14)).

$$\text{LCOM} = \frac{\left(\sum CAPEX_{plant} + \sum CAPEX_{H_2,prod.} + \sum CAPEX_{power,gen.} + \sum CAPEX_{storages}\right) \cdot CRF + \sum O\&M_{fixed} + \sum O\&M_{variable}}{MeOH_{prod.}} [€\ \text{per t}] \quad (13)$$

$$CRF = \left(\sum_{t=1}^{lt} \frac{1}{(1+r)^t}\right)^{-1} = \frac{r \cdot (1+r)^{lt}}{(1+r)^{lt} - 1} \quad (14)$$

The Net Present Value (NPV) is calculated with eqn (15) assuming an income tax rate between 0 and 30%. The Internal Rate of Return (IRR) represents the discount rate that results in a zero NPV.

$$NPV = \sum_{t=1}^{lt} \frac{(Revenues - Cost) \cdot (1 - tax)}{(1+r)^t} - CAPEX \quad (15)$$

The Profitability Index (PI) is defined as the ratio between the present value of the future cash flows (NPV + CAPEX) and the

total system CAPEX (eqn (16)). An investment is therefore considered profitable when the PI exceeds 1.0, as this indicates that the present value of future cash flows is sufficient to recover the initial capital expenditure.

$$\mathrm{PI} = 1 + \frac{\mathrm{NPV}}{\mathrm{CAPEX}} \tag{16}$$

The LCOE calculation for PV and wind (eqn (17)) compares the total annualised costs (encompassing both amortised CAPEX and OPEX) against the total energy generated by the plants annually. A separate metric, the cost of used renewable energy ($\mathrm{LCOE_u}$), is defined for the energy actually consumed by the chemical island, thereby disregarding the value of any curtailed surplus electricity (eqn (18)).

$$\mathrm{LCOE}_{\mathrm{PV\ or\ Wind}} = \frac{(\mathrm{CAPEX}_{\mathrm{PV\ or\ Wind}}) \times \mathrm{CRF} + \text{fixed O\&M} + \text{var O\&M}}{\mathrm{EE}_{\mathrm{PV\ or\ Wind}}} \left[\frac{€}{\mathrm{MWh}}\right] \tag{17}$$

$$\mathrm{LCOE_u} = \frac{(\mathrm{CAPEX_{PV}} + \mathrm{CAPEX_{bat}} + \mathrm{CAPEX_{wind}}) \cdot \mathrm{CRF} + \sum \text{fixed O\&M} + \sum \text{var O\&M}}{\sum_{t=1}^{8760} (E_{\mathrm{ren},2}(t) + b_2(t))} \left[\frac{€}{\mathrm{MWh}}\right] \tag{18}$$

3 Results

3.1 Process analysis

Table 4 presents the main technical results for the bio-e-MeOH plant at its three key operating points, comparing them against a benchmark case utilising a conventional Fired Tubular Reformer (FTR).[24] The eSMR consistently achieves a high CH_4 conversion of 95.8–97.3%.

In the base load mode, the raw syngas stoichiometric module is 1.17. Due to the CO_2-rich recycle stream, the M at the reactor inlet drops to −0.50. This hydrogen-deficient feed limits the single-pass methanol yield to 7.0%, although the overall global yield remains high at 71.1%. It is worth noting that the hydrogen-based yields are significantly higher (37.0% single-pass and 82.8% overall), confirming that hydrogen is the limiting reactant in this scenario. Notably, the base load carbon efficiency is 70.1%, significantly higher than the benchmark's 49.8%, which is heavily penalised by the need to combust 33.9% of the incoming biogas in the furnace to sustain the reformer. When accounting for its specific electricity consumption (3.25 $\mathrm{kWh/kg_{MeOH}}$), the base load's overall methanol production efficiency is 67%, with associated biogenic CO_2 emissions of 0.497 $\mathrm{kg_{CO_2}/kg_{MeOH}}$.

In the enhanced MeOH mode, hydrogen addition from the electrolyser is used to adjust the syngas stoichiometric module to an optimal value of 2.1. This, combined with a hydrogen-rich recycle stream, brings the reactor inlet M to 8.50. The single-pass yield increases tenfold to 66.8%, and the global methanol yield reaches 98.0%. Conversely, the hydrogen-based yields are lower compared to the base load operating point, indicating that carbon acts as the limiting reactant in this operating mode. As a result, the total carbon efficiency increases to 95.9% and the biogenic CO_2 emissions reduce to 0.050 $\mathrm{kg_{CO_2}/kg_{MeOH}}$.

The high carbon utilization comes at the cost of significant electricity consumption (5.46 $\mathrm{kWh/kg_{MeOH}}$), primarily for the electrolyser. This results in a methanol production efficiency of 62%, which is lower than the base load case. Finally, in the electric neutral mode, 62% of the biogas is diverted to the ICE. This involves a drop in the carbon efficiency to 26.5% and a rise in specific biogenic CO_2 emissions to 3.737 $\mathrm{kg_{CO_2}/kg_{MeOH}}$.

Table 5 presents a detailed breakdown of the total installed CAPEX for the chemical island, segmented into its three main process sections. To ensure a rigorous and fair comparison with the benchmark FTR-based plant from ref. 24, a thorough cost harmonisation was performed. The methanol reactor cost in ref. 24 was re-estimated using the same methodology applied in ref. 25. For all other conventional components (*e.g.*, heat exchangers, columns, and compressors), the cost estimations from ref. 24 were adopted and escalated to €2023 using the Chemical Engineering Plant Cost Index (CEPCI).[39] For the eSMR, the model described in ref. 36 has been adopted. For the benchmark FTR, cost is estimated with the function proposed by Herz *et al.*[58] Electrified reforming significantly simplifies the syngas generation section by eliminating the furnace and its associated flue-gas heat recovery system. The cost of the eSMR unit is estimated to be approximately one-third the cost of the conventional FTR. This simplification, combined with reduced expenses for associated heat exchangers and auxiliaries, leads to a 52% reduction in CAPEX for the entire syngas generation section (dropping from 39% to 16% of the total plant cost). This cost advantage is counterbalanced by the downstream process. Because the eSMR plant processes 100% of the biogas to chemical conversion (unlike the FTR benchmark, which combusts 34% of it), the methanol synthesis loop must be sized to handle a larger syngas throughput. This directly results in higher costs for the syngas

Table 4 Main technical results of the chemical island working in different operating points and comparison with the benchmark with a Fired Tubular Reformer (FTR)

			Bio-e-MeOH with eSMR		
Operating points		Benchmark with an FTR[24]	Electric neutral	Base load	Enhanced MeOH
Biogas to reformer furnace	%	33.9%	—	—	—
Biogas to ICE	%	—	62%	—	—
Steam to CH_4 ratio in eSMR	mol_{CH_4}/mol_{H_2O}	3.86	3.80	4.69	4.69
CH_4 conversion in eSMR	%	95.8%	95.8%	97.3%	97.3%
Stoichiometric module (M)	—	1.35	1.16	1.17	2.11
Recycle ratio	—	5.00	10.12	4.78	3.27
Syngas module after recycle	—	−0.39	−0.65	−0.50	8.50
CO/CO_2 ratio at the reactor inlet	—	0.18	0.16	0.14	0.57
CH_4 at the reactor inlet	$\%_{mol}$	9.6%	15.4%	10.1%	5.1%
MeOH reactor: GHSV	$Nm^3\ h^{-1}\ m_{CAT}{}^{-3}$	4003	2896	4035	4001
Single pass methanol yield	%	8.4%	3.5%	7.0%	66.8%
Global methanol yield	%	78.1%	71.1%	71.6%	98.0%
Single pass methanol yield (H_2 base)	%	—	32.5%	37.0%	14.6%
Global methanol yield (H_2 base)	%	—	85.4%	82.8%	73.5%
Carbon efficiency	%	49.8%	26.5%	70.1%	95.9%
Methanol production energy ratio	%	70.0%	40.2%	106.9%	146.9%
Methanol production efficiency	%	66%	40%	67%	62%
Biogenic CO_2 emitted	kg_{CO_2}/kg_{MeOH}	1.37	3.737	0.497	0.050
Electricity consumption breakdown					
Biogas compressor	kWh/kg_{MeOH}	0.128	0.131	0.129	0.095
eSMR	kWh/kg_{MeOH}	—	2.400	2.454	1.793
Syngas compressor	kWh/kg_{MeOH}	0.330	0.404	0.409	0.299
Recycle compressor	kWh/kg_{MeOH}	0.031	0.086	0.043	0.038
Blowers, pumps and coolers	kWh/kg_{MeOH}	0.062	0.009	0.013	0.008
Heat pump (COP = 3)	kWh/kg_{MeOH}	—	0.544	0.206	0.206
Hydrogen compressor	kWh/kg_{MeOH}	—	—	—	0.047
Electrolyser (68% efficiency)	kWh/kg_{MeOH}	—	—	—	2.975
Biogas ICE	kWh/kg_{MeOH}	—	−3.58	—	—
Total	kWh/kg_{MeOH}	0.551	0.000	3.253	5.460

Table 5 CAPEX breakdown and comparison with the benchmark using a Fired Tubular Reformer (FTR)

CAPEX breakdown k€	Unit	FTR-based plant (adapted from ref. 24)		eSMR-based plant	
Biogas compressor	k€	1238	7%	1595	8%
Syngas generation	k€				
Heat exchangers		2861	16%	2052	10%
Auxiliaries		665	4%	115	1%
eSMR		—	—	1246	6%
FTR		3614	20%	—	—
Total syngas generation		7140	39%	3413	16%
Methanol synthesis	k€				
Syngas compressor		2425	13%	3527	17%
Recycle compressor		792	4%	1052	5%
Heat exchangers		850	5%	1430	7%
MeOH reactor		4208	23%	6944	33%
Boiler		—	—	1818	9%
Auxiliaries		82	0%	204	1%
Total MeOH synthesis		8358	45%	14 975	71%
Methanol purification	k€				
Heat exchangers		58	0%	48	0%
First distillation column		492	3%	340	2%
Second distillation column		1172	6%	768	4%
Total MeOH purification		1722	9%	1156	5%
Total CAPEX	**k€**	**18 458**	**100%**	**21 140**	**100%**
Specific CAPEX [€ $kW_{MeOH}{}^{-1}$]		**1318**		**1084**	

compressor, recycle compressor, and the methanol reactor itself. Furthermore, this section now includes a boiler (9% of total CAPEX) to generate steam from purge gases. Consequently, the total CAPEX for the methanol synthesis section increases by 80%. Overall, these trade-offs result in a total plant CAPEX for the eSMR system that is 15% higher than the FTR benchmark. However, this increased investment yields a proportionally larger methanol output. When normalized to the methanol production capacity, the eSMR plant is 18% cheaper than the benchmark (1084 € kW_{MeOH}^{-1}, *vs.* 1318 € per kW_{MeOH}^{-1}).

3.2 Optimization results

To assess the impact of different variable renewable energy profiles, techno-economic optimisation was performed for two locations: (i) Sicily (South Italy), representing a region with high solar and good on-shore wind resources; and (ii) Denmark, representing a region dominated by high-yield off-shore wind resources but with limited solar irradiation. The respective capacity factors (CFs) for PV and wind in both locations are presented in Table 6. This table also lists the corresponding Levelised Cost of Electricity (LCOE) for each technology under the different economic scenarios investigated in this study.

3.2.1 Hourly behaviour of flexible systems. The hourly energy balance for the enhanced flexibility plant is presented in Fig. 3, showing a representative 20 day period in South Italy, starting from January 1st. Positive areas in the top plot represent power generation (PV, wind, and BESS discharge), while negative areas represent power consumption by the chemical plant, electrolyser, BESS charging and energy curtailment. The bottom plot shows the hourly state of charge of material storage units. During periods of high renewable availability, the plant ramps up syngas production by drawing biogas from its storage. This is clearly visible in the biogas (light green line) and syngas (dark green line) storage levels, which operate in inverse daily cycles: the biogas tank empties to feed the eSMR, and the resulting syngas surplus is stored. Conversely, when renewable availability is scarce, syngas production is reduced (down to the minimum load of 25% of nominal capacity), and the biogas tank is refilled.

Table 6 Capacity factors and LCOE of PV and wind for the selected locations in short-term and long-term scenarios

Location	unit	South Italy	Denmark
Wind			
Capacity factor	%	27.3%	55.1%
LCOE wind, short-term	€ MWh^{-1}	81.7	78.4
LCOE wind, long-term	€ MWh^{-1}	65.8	70.4
LCOE wind, long-term visionary	€ MWh^{-1}	50.3	67.3
PV			
Capacity factor	%	18.9%	9.9%
LCOE PV, short-term	€ MWh^{-1}	57.3	150.2
LCOE PV, long-term	€ MWh^{-1}	48.2	92.6
LCOE PV, long-term visionary	€ MWh^{-1}	22.1	42.3

Simultaneously, the hydrogen storage (red line) is filled during peaks of renewable generation and is then drawn down when power is scarce, ensuring a stable H_2 supply to the synthesis loop. When the hydrogen storage is empty and insufficient power is available for electrolysis, the plant reverts to the base load operating mode. In this condition, the plant operates without H_2 addition, leading to a decrease of methanol production. In the specific timeframe considered, the ICE is never dispatched; therefore, the plant operation alternates between the base load and enhanced MeOH modes.

Observing the annual behaviour of the storage units in Fig. 4, it is evident that the crude methanol tank (purple line) operates on a different timescale than the other buffers. While it absorbs short-term (daily and weekly) variability, its overall state of charge follows a seasonal cycle. In the Italian case, for example, it progressively fills during the sunniest months and is depleted during the winter, thereby guaranteeing a constant feed to the purification section year-round. Fig. 4 also highlights the impact of removing the intermediate storage options. In the "flexible" case (Fig. 4a and c), where syngas and hydrogen buffers are excluded, the optimized system compensates with significantly larger biogas and crude methanol storage capacities. This contrasts with the "enhanced flexibility" case (Fig. 4c and d), where the daily variability is handled by the syngas and hydrogen tanks, allowing the seasonal methanol tank to operate with a similar profile but at a reduced volume. In the Danish scenario, the multi-day variability of the off-shore wind requires larger energy reserves compared to the daily cycles of solar PV in Italy. Consequently, the seasonal methanol storage is consistently larger (7000–8000 MWh). Although the enhanced flexibility configuration leads to a reduction in both methanol and biogas storage capacities, this effect is significantly less pronounced in Denmark than in Italy.

3.2.2 Impact of flexibility. Fig. 5 presents the annual energy balances for the Italian and Danish systems across different methanol selling prices under the long-term scenario. As the methanol selling price increases, it becomes more profitable to maximise production. Consequently, reliance on the ICE decreases while the total electricity consumed (and therefore the required renewable capacity) increases. Notably, the electrolyser becomes economically viable and is installed only at high selling prices (*i.e.*, 1100 € t^{-1}). Furthermore, compared to inflexible setups, operational flexibility allows the plant to reduce the installed renewable capacity for a given energy demand, significantly decreasing both energy curtailment and BESS utilisation.

Fig. 6 illustrates the trade-off between methanol production costs and carbon efficiency. Inflexible configurations consistently yield the highest production costs across all scenarios and are heavily penalised in terms of carbon efficiency. At the lowest selling price, their efficiency drops to 26–32% due to excessive biogas combustion for power generation, peaking at only 62–67% even at higher prices. In contrast, in both the "flexible" and "enhanced flexibility" configurations, as the methanol selling price increases, the profitable integration of the electrolyser allows these systems to substantially boost their carbon efficiency, surging from 51–55% at 500 € t^{-1} to 87–92%

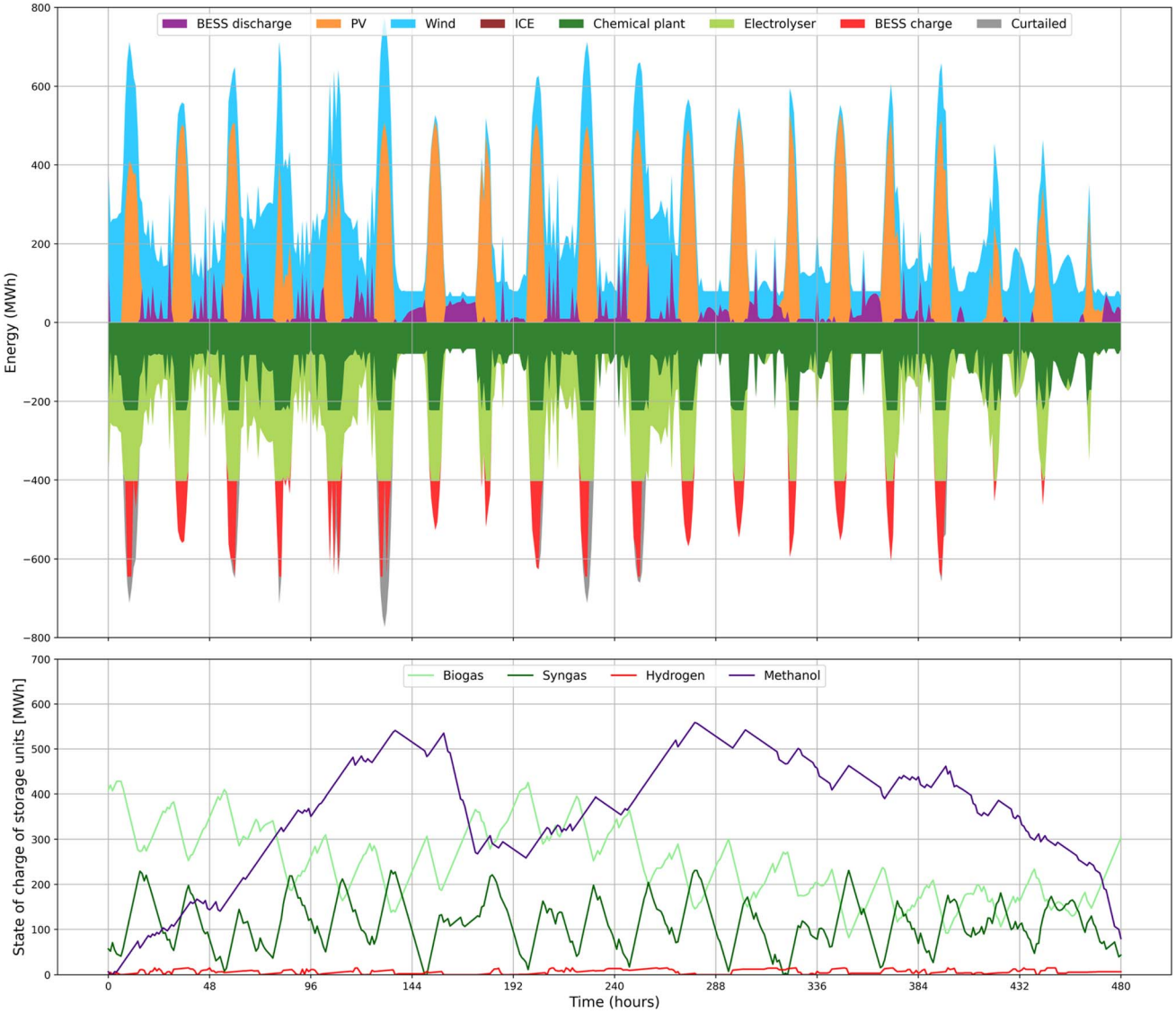

Fig. 3 Hourly energy balance profiles for the long-term scenario in Italy, with enhanced flexibility and a methanol selling price of 1100 € t^{-1} (above) and state of charge of storage units (below).

at 1400 € t^{-1}, albeit at the expense of higher specific production costs. Notably, the differences in production cost between the "flexible" and "enhanced flexibility" setups are minimal (up to 3%). This clearly indicates that intermediate storage for biogas and crude methanol alone is sufficient to capture the vast majority of the economic benefits associated with operational flexibility. An in-depth discussion and all results concerning the different degrees of flexibility are reported in the SI.

3.2.3 Impact of economic scenarios. This section discusses the impact of the three economic scenarios on the optimal system design, starting with the annual energy balances shown in Fig. 7 for the "flexible" case. The economic assumptions fundamentally alter the plant's design and operational strategy. As renewable technologies become cheaper, combusting biogas for power generation becomes uncompetitive. Consequently, the use of the ICE (orange bars) is drastically reduced in the "long-term visionary" scenarios, in favour of installing larger PV and wind capacities, along with an increased battery use.

The viability of the electrolyser (light green bars) is the most critical difference. In the "short-term" and "long-term" scenarios, its high CAPEX (1000–1300 € kW^{-1}) means it is only installed when methanol prices are high (*e.g.* higher than 1000 € t^{-1}). However, in the "long-term visionary" scenario, the significantly lower CAPEX of electrolysis systems (360 € kW^{-1}) makes it a profitable investment at much lower prices, appearing already at 500 € t^{-1}. This "visionary" assumption encourages an oversizing of renewable capacity, particularly in the Italian case, where cheap solar (yellow bars) is scaled up significantly. This strategy accepts high energy curtailment (grey bars) as a trade-off for maximising methanol production with reduced costs of renewable technologies and electrolysis systems.

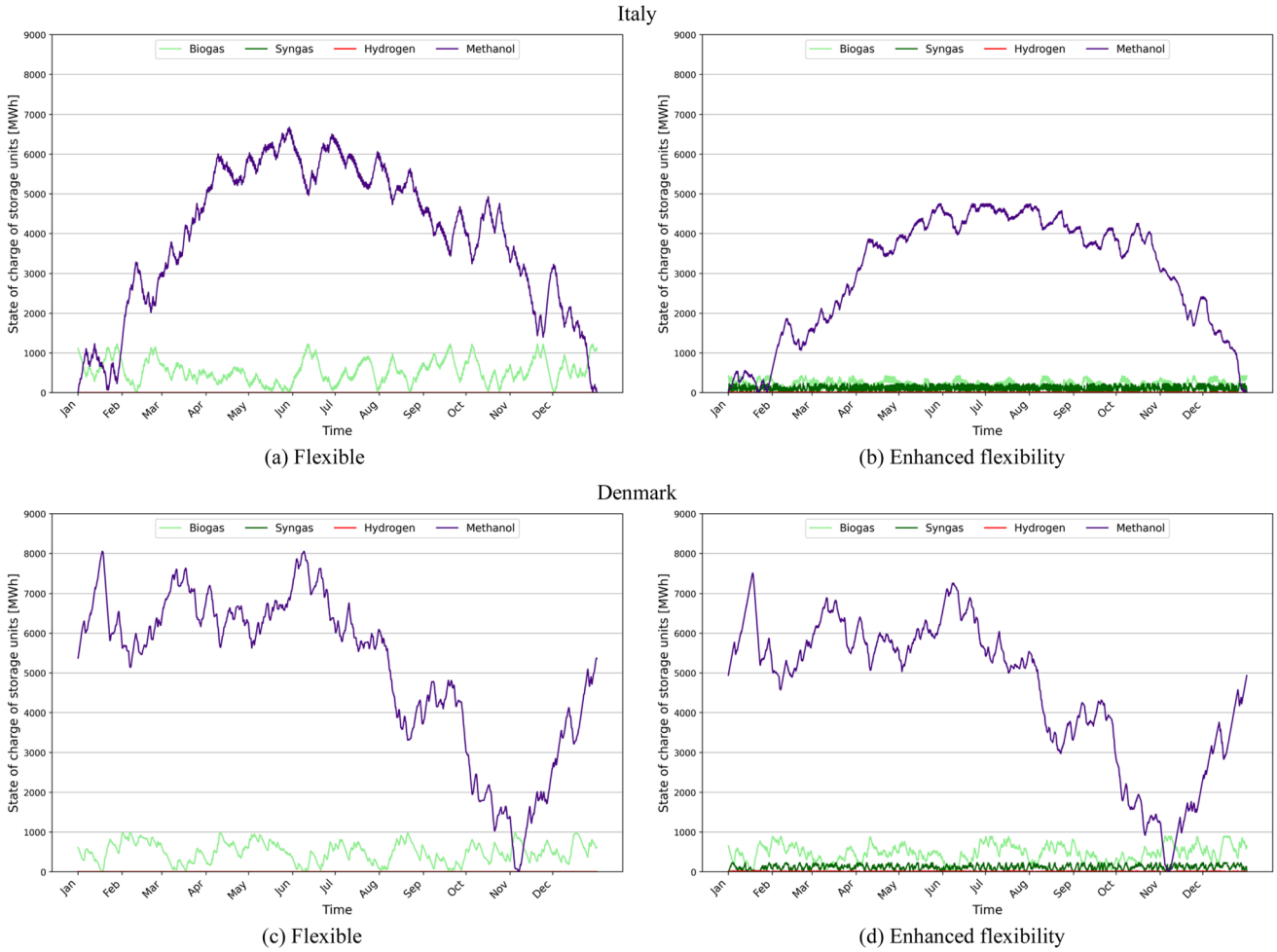

Fig. 4 Annual state of charge profiles of gas/liquid storage units of the bio-e-methanol process for a methanol selling price of 1100 € t^{-1}, in the long-term scenario: (a) flexible system in Italy; (b) enhanced flexibility system in Italy; (c) flexible system in Denmark; and (d) enhanced flexibility system in Denmark.

The methanol production cost breakdown for each economic scenario is presented in Fig. 8, while Fig. 9 plots the production cost (solid lines, left axis) and annual carbon efficiency (dashed lines, right axis) as a function of the methanol selling price.

As expected, the total cost generally decreases as the underlying renewable technology costs fall, with the "long-term visionary" scenario (orange lines in Fig. 9) consistently achieving the lowest production cost and the highest carbon efficiency. In this scenario, both production cost and carbon efficiency show a monotonic rise as the selling price increases. In contrast, the "short-term" (blue) and "long-term" (green) scenarios exhibit a minimum in their methanol production cost curves.

At 1100 € t^{-1}, the production costs of the "short-term" and "long-term" scenarios converge. At this specific price point, the "long-term" case leverages its cheaper renewable costs to invest more heavily in PV, wind, and electrolyser capacity (as seen in its cost bar composition in Fig. 8) to boost the total annual production. As a result, the "long-term" case achieves a significantly higher carbon efficiency for essentially the same production cost. As the price increases further to 1400 € t^{-1}, the "short-term" case also installs the electrolyser, causing a divergence of the production cost curves.

Finally, Fig. 10 illustrates the project's economic viability, plotting the Profitability Index (PI) and Internal Rate of Return (IRR) for the three economic scenarios as a function of methanol selling price (within a 0–30% taxation range). At a low selling price of 500 € t^{-1}, all configurations are economically unviable (PI < 1), which is consistent with the finding that their production costs are well above this selling price. The "long-term visionary" scenario (orange lines) shows the most dramatic response to price. In Italy (Fig. 10a), the low assumed costs for PV and electrolysers enable a steep increase in profitability, with the PI rising from 1.4–1.9 (at 800 € t^{-1}) to 2.5–3.6 (at 1400 € t^{-1}). This potential is constrained in Denmark (Fig. 10c), where the higher cost of off-shore wind limits the maximum PI to a lower 2.0–2.8 range.

In contrast, the "short-term" scenario in Italy (blue lines in Fig. 10a) exhibits a critical trend: the PI increases as the price rises to 1100 € t^{-1}, where it peaks, but then slightly declines at 1400 € t^{-1}. This is because the increase in the NPV (higher

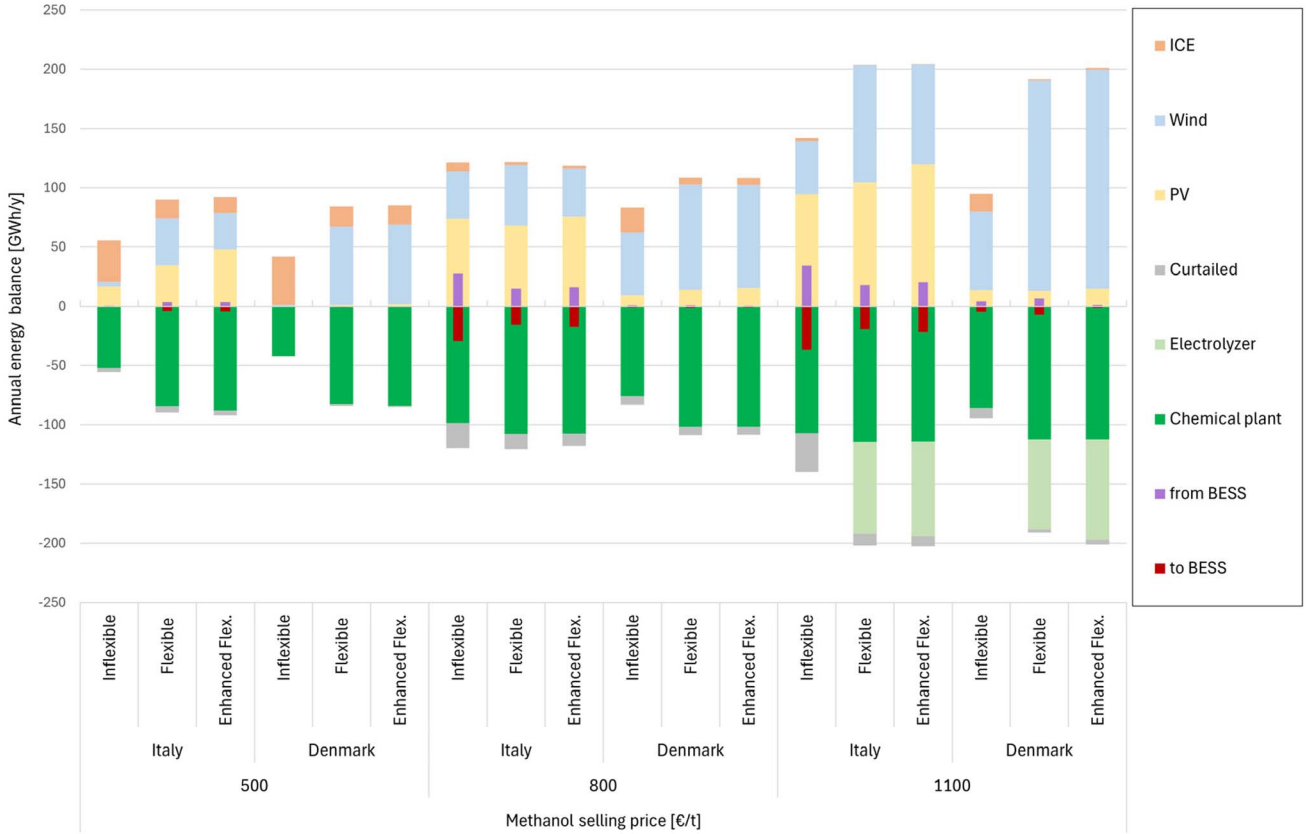

Fig. 5 Annual energy balance of the bio-e-MeOH system for different degrees of flexibility, in Italy and Denmark, for different methanol selling prices, in the long-term scenario.

production of methanol sold at a higher price) is more than offset by the sharp rise in the investment costs, driven by the installation of the electrolysis system and the related increase in installed renewable capacity. This flattening effect, which limits profitability, is not observed in the "long-term" scenarios where electrolysis is much cheaper.

The main optimisation results across the different economic scenarios are presented in Table 7 for the "flexible" case, at varying methanol selling prices in South Italy (an equivalent table for Denmark is included in the SI). The reduced cost of renewable technologies in the long-term scenarios makes it profitable to install significantly more capacity. For example, with a methanol selling price of 800 € t^{-1}, the optimal installed PV capacity increases from 22 MW in the "short-term" scenario to 89 MW in the "long-term visionary" scenario. A 26 MW electrolysis system is also installed, which in turn boosts the relative size of the

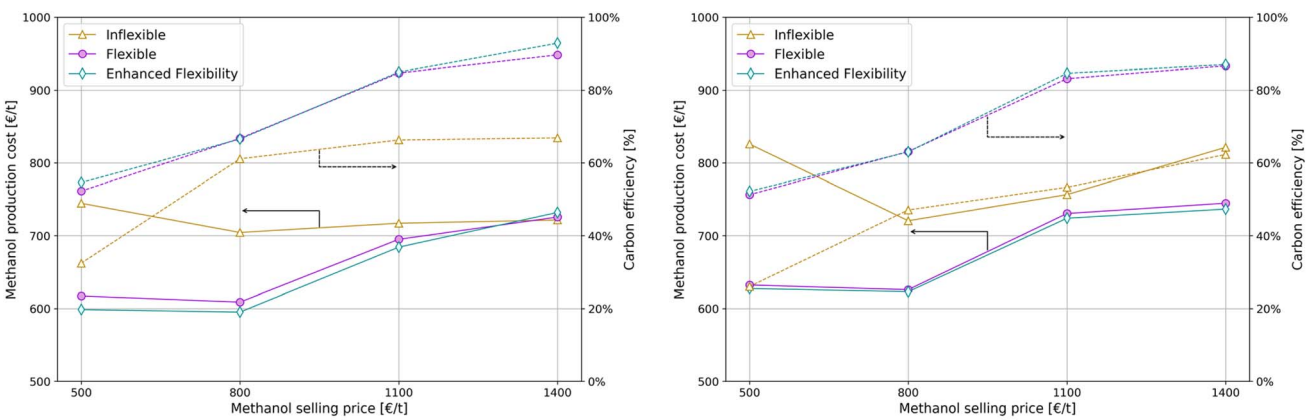

(a) Italy (b) Denmark

Fig. 6 Methanol production cost and carbon efficiency as a function of methanol selling price in Italy (a) and Denmark (b), in the long-term scenario.

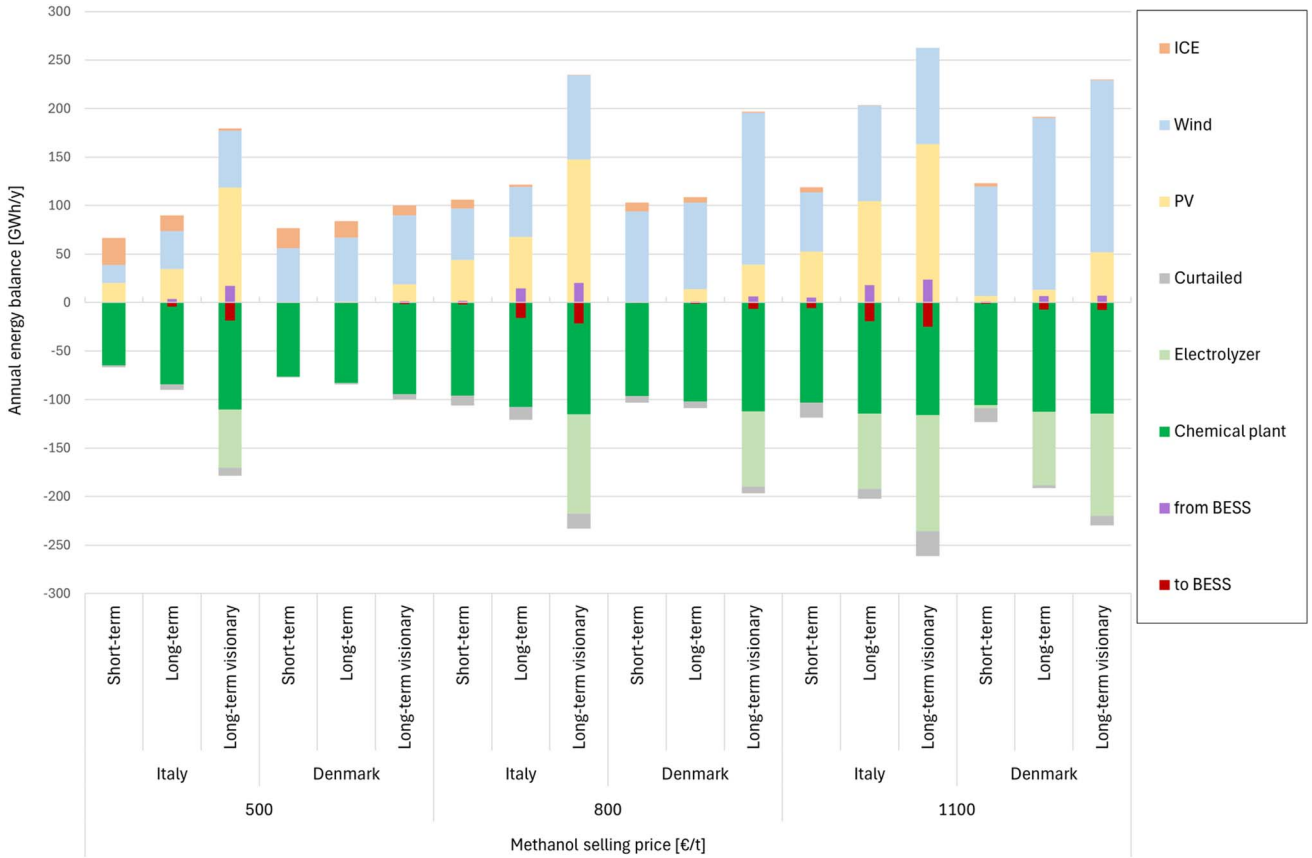

Fig. 7 Annual energy balance of the bio-e-MeOH system in different economic scenarios for "flexible" plants, in Italy and Denmark, for different methanol selling prices.

syngas generation section (from 145% to 165%) and drives a 50% increase in annual methanol production (from 29.0 kt year^{-1} to 43.7 kt year^{-1}) and carbon efficiency (from 60% to 90%).

3.2.4 Comparison between eSMR and FTR. Fig. 11 presents the results of the comparative analysis between the flexible bio-e-methanol process, across the various investigated economic scenarios, and the FTR benchmark. For the benchmark case, an electricity cost range of 100–200 € MWh^{-1} is considered (represented by the light blue shaded area). To ensure a fair comparison between the two technologies, the NPV and IRR for the eSMR configuration were calculated by exclusively considering the CAPEX of the chemical island and the storage units. In this evaluation, the cost of electricity is accounted for as an OPEX, charged at a price equivalent to the $LCOE_u$ previously derived from the optimisation model. The economic results in this case exclude taxation.

Regarding the NPV, the competitiveness of the eSMR-based process is strictly linked to the methanol selling price. In the "long-term" scenario, the eSMR configuration yields a higher NPV than the FTR benchmark when methanol prices exceed approximately 800 € t^{-1}. In the "long-term visionary" scenario, this break-even threshold decreases to roughly 550 € t^{-1}. Conversely, in terms of IRR, the FTR benchmark exhibits superior performance. This disparity arises from the operational strategy of the electrified systems: as the methanol selling price increases, the optimisation framework drives higher investments in renewable energy generation and electrolysis to maximise production. In contrast, the benchmark production capacity remains constant; consequently, its IRR increases linearly with the rising methanol market value. It is worth noting that the strong economic competitiveness of the FTR benchmark is primarily driven by the assumed cost of biogas (34 € MWh^{-1}), which is significantly lower than the $LCOE_u$ of the renewable plants with BESSs, ranging from approximately 45 € MWh^{-1} in the long-term visionary scenarios to about 85 € MWh^{-1} in the short-term scenarios.

3.2.5 Project scale and electricity price. The previous sections analysed a large-scale system processing 21 MW (3915 Nm^3 h^{-1}) of biogas, highlighting how the biogas cost significantly impacts the overall economics. However, typical anaerobic digesters could operate at much smaller capacities. As emphasised by the Biomethane Industrial Partnership©, while large-scale plants may incur higher transport costs due to longer collection distances, this is more than offset by the economies of scale associated with the capital investment, ultimately leading to a lower production cost.[59] In this study, a biogas production cost of 34 € MWh^{-1} was assumed for the large-scale reference plant.[60] To model the impact of scaling, the "two-thirds power law" was applied to the chemical island CAPEX. For the biogas production cost, the exponential scaling law was applied exclusively to the 50% CAPEX-dependent

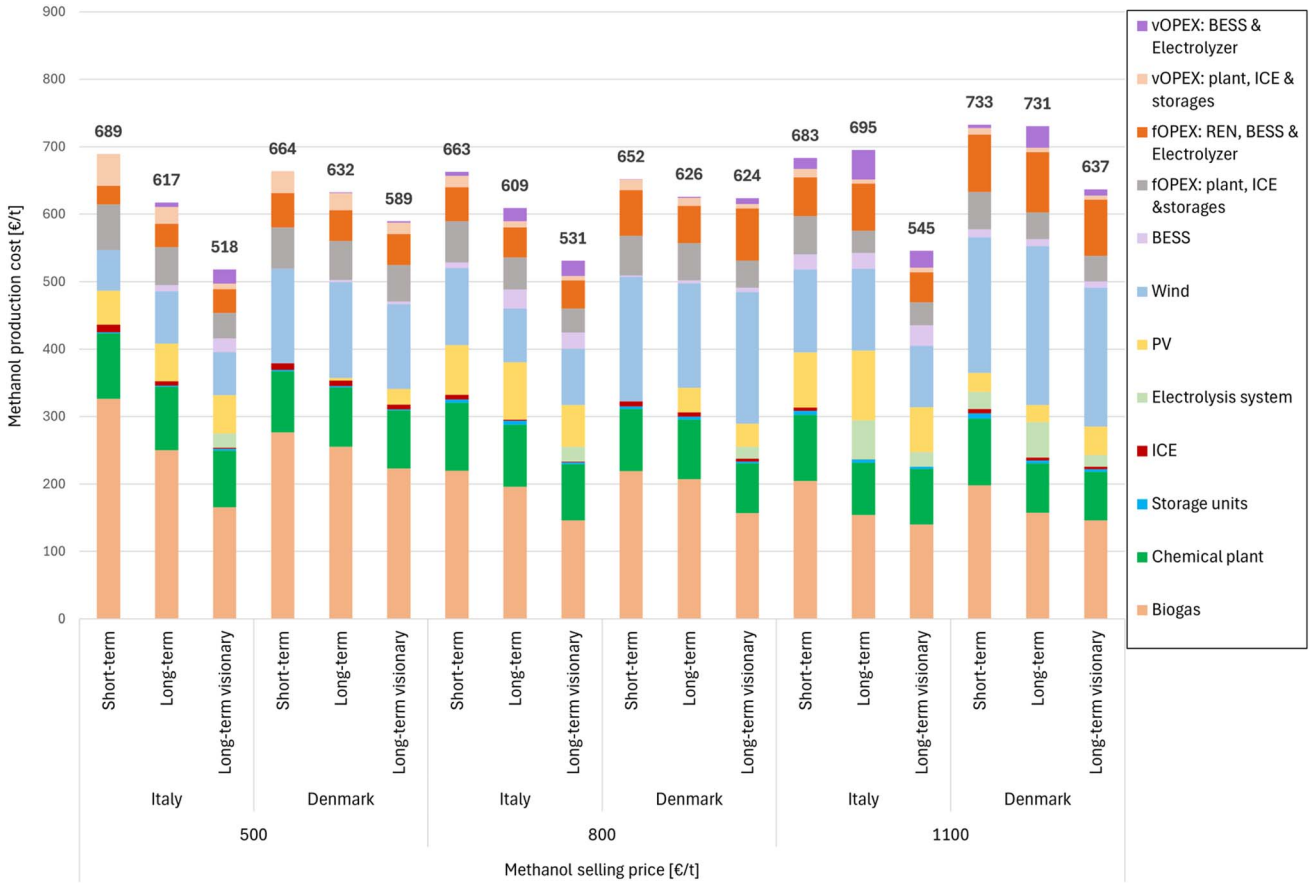

Fig. 8 Methanol production cost (LCOM) in different economic scenarios for "flexible" plants, in Italy and Denmark, for different methanol selling prices.

fraction, leaving the remaining scale-independent 50% constant.[59] This results in a biogas cost varying from 34 € MWh^{-1} at large scale to 54 € MWh^{-1} at small scale, consistent with IEA data.[1,60] Conversely, no economies of scale were assumed for the modular renewable technologies. Fig. 12 presents the results of this analysis for the optimal "flexible" configuration in Italy, with a methanol selling price of 800 € t^{-1}. The impact of economies of scale is substantial: the methanol production cost rises sharply from 529–663 € t^{-1} for large-scale plants to 760–1009 € t^{-1} for small-scale plants (2.1 MW, or 391 Nm^3 h^{-1}), which are representative of agricultural biodigesters in Italy. Consequently, to bridge the cost gap with

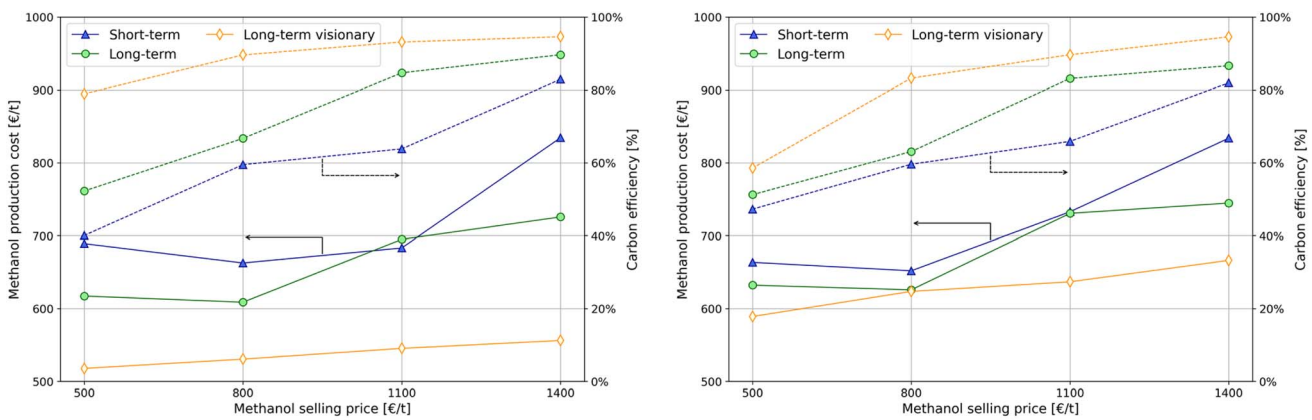

Fig. 9 Methanol production cost and carbon efficiency as a function of methanol selling price in Italy (a) and Denmark (b), for the "flexible" plant.

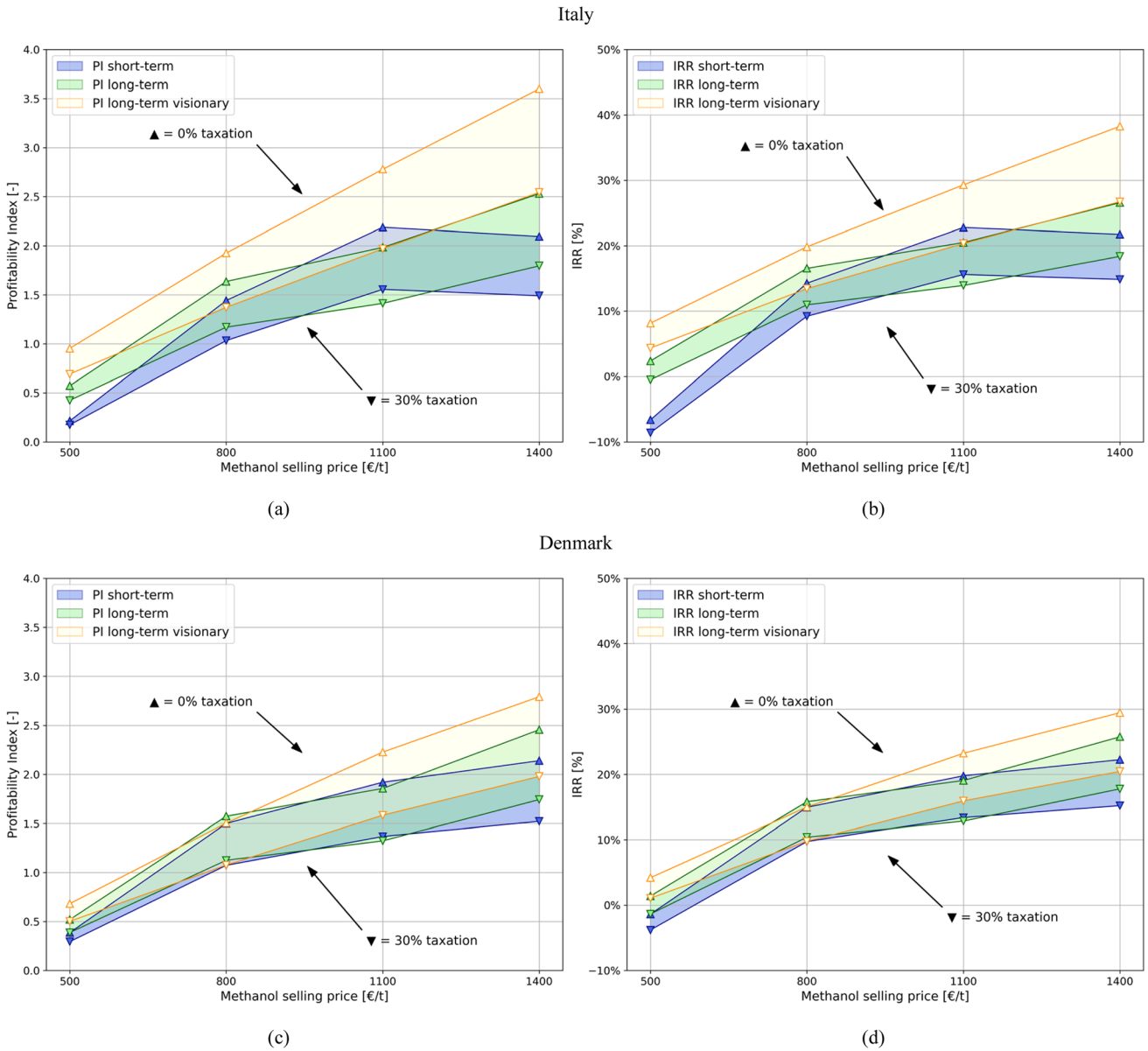

Fig. 10 Profitability Index (PI) and Internal Rate of Return (IRR) for "flexible" plants in different economic scenarios, as a function of methanol selling price in Italy (a) and (b) and Denmark (c) and (d).

fossil-based methanol (100–500 € t^{-1}),[42,61] investing in centralised, large-scale systems is essential. The figure also includes a comparison (light blue area) with benchmark bio-methanol production *via* a conventional Fired Tubular Reformer (FTR). The FTR route generally yields a lower production cost and significantly lower electricity consumption, which is primarily limited to reactant compression.

Evaluated on an energy basis, the production cost of bio-e-methanol thus varies between 91–114 € MWh^{-1} at large scale and 130–174 € MWh^{-1} at small scale. These values are notably higher than those of bio-methane, which has an average production cost in Europe ranging between 55 and 91 € MWh^{-1}.[59] Consequently, the competitiveness of bio-e-methanol is highly context-dependent and relies on a higher selling price that recognises the higher value of methanol compared to methane.

3.2.6 Emissions. The environmental performance of the optimal system configurations is analysed in Fig. 13, which plots the specific equivalent CO_2 emissions per MJ of methanol produced (LHV basis) for the "flexible" case in South Italy, under long-term economic assumptions. As detailed in the Methodology section, the analysis considers two boundary scenarios: a "low emission scenario" (optimistic assumptions for embodied emissions and 0.5% methane slip) and a "high emission scenario" (conservative assumptions and 2% methane slip). The breakdown identifies methane slip (orange area) as the dominant contributor to the total carbon footprint, particularly in the high emission scenario.

Table 7 Main optimisation results for "flexible" plants in South Italy as a function of methanol selling price and in different economic scenarios

Location		South Italy								
MeOH selling price		500			800			1100		
Cost scenario		Short-term	Long-term	Long-term visionary	Short-term	Long-term	Long-term visionary	Short-term	Long-term	Long-term visionary
Biogas input	$Nm^3\ h^{-1}$	3915								
Biogas thermal input	MW_{LHV}	21.4								
Chemical island relative size[a]										
Syngas generation	%	73%	107%	138%	145%	149%	165%	152%	135%	169%
MeOH synthesis	%	73%	108%	139%	145%	150%	165%	153%	136%	169%
Installed capacity										
Biogas ICE	MW_{el}	4.52	3.25	1.18	4.04	1.06	0.62	3.27	0.10	—
PV	MW_{el}	12.21	21.00	71.42	26.69	41.00	88.89	31.90	63.06	98.61
Wind	MW_{el}	7.83	16.36	24.70	22.08	21.49	36.41	25.46	41.35	41.48
Electrolyzer	MW_{el}	—	—	22.02	—	—	26.22	—	21.57	26.87
BESS	MWh_{el}	—	18.49	63.51	9.32	73.62	84.92	26.47	76.43	110.07
BESS eq. cycles	—	—	223	291	214	214	256	216	250	228
Storages										
Biogas	m^3	2353	3612	14 674	19 946	24 978	16 342	26 706	28 453	23 076
Biogas STH	h	4.7	7.3	29.5	40.1	50.2	32.8	53.6	57.1	46.3
Methanol	m^3	484	1155	1344	1403	1043	1213	1298	1864	1190
Methanol STH	h	55.0	131.2	152.7	159.4	118.5	137.8	147.5	211.9	135.3
Capacity factors										
PV	% h $year^{-1}$	19%	19%	19%	19%	18%	18%	18%	19%	18%
Wind	% h $year^{-1}$	24%	24%	24%	22%	22%	24%	21%	25%	23%
ICE	% h $year^{-1}$	70%	57%	21%	26%	25%	1%	18%	4%	0%
Electrolyser	% h $year^{-1}$	0%	0%	31%	0%	0%	44%	0%	41%	51%
Production										
Methanol	t $year^{-1}$	19 555	25 509	38 531	29 050	32 573	43 735	31 164	41 339	45 467
Carbon efficiency	%	40%	52%	79%	60%	67%	90%	64%	85%	93%
Economics										
TAC	M€ $year^{-1}$	3.70	2.99	0.69	−3.99	−6.23	−11.78	−12.99	−16.74	−25.22
$LCOE_u$	€ MWh^{-1}	72.6	68.4	42.9	84.2	78.8	44.6	95.3	69.6	47.4
EE curtailed	%	4.9%	7.2%	4.6%	10.3%	10.9%	6.6%	13.5%	5.0%	9.7%
LCOM	€ t^{-1}	702	630	518	676	621	531	696	695	545
NPV (0% tax)	M€	−33.04	−26.07	−4.44	38.61	59.25	110.54	121.43	155.71	234.09
NPV (30% tax)	M€	−34.72	−35.04	−29.17	2.90	15.79	44.44	56.81	65.35	127.58
IRR (0% tax)	%	−7%	2%	8%	14%	17%	20%	23%	21%	29%
IRR (30% tax)	%	−9%	−1%	4%	9%	11%	13%	16%	14%	20%
PI (0% tax)	—	0.21	0.57	0.95	1.44	1.64	1.93	2.19	1.98	2.78
PI (30% tax)	—	0.17	0.42	0.69	1.03	1.17	1.37	1.56	1.41	1.97

[a] Percentage values are expressed relative to a chemical island sized to process the nominal biogas production rate directly.

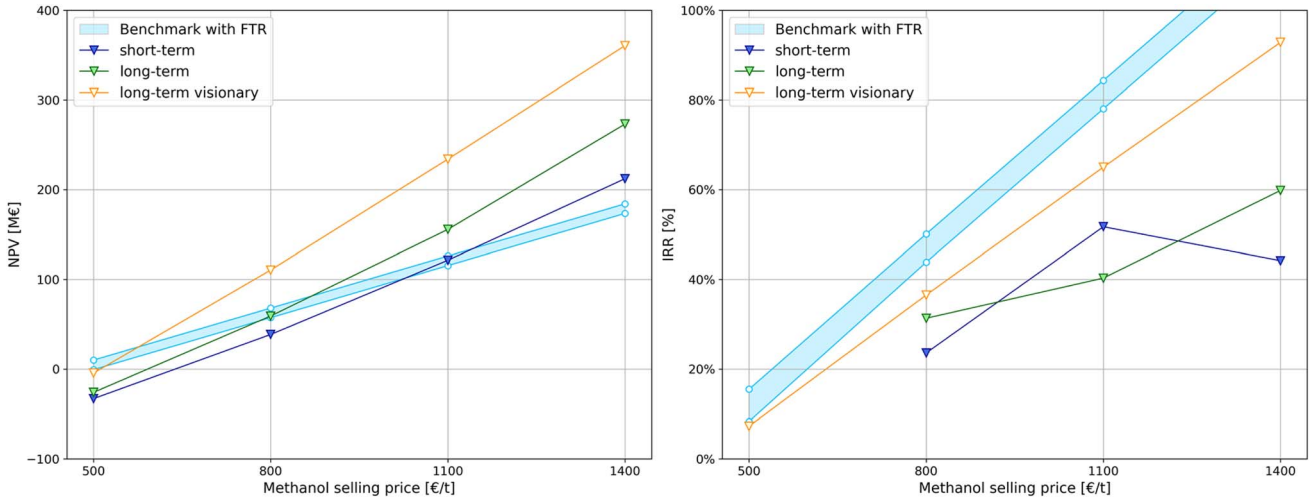

Fig. 11 Comparison between eSMR and FTR for bio-e-methanol production, considering the NPV (left) and the IRR (right). The results for the eSMR case are presented in the various economic scenarios analysed.

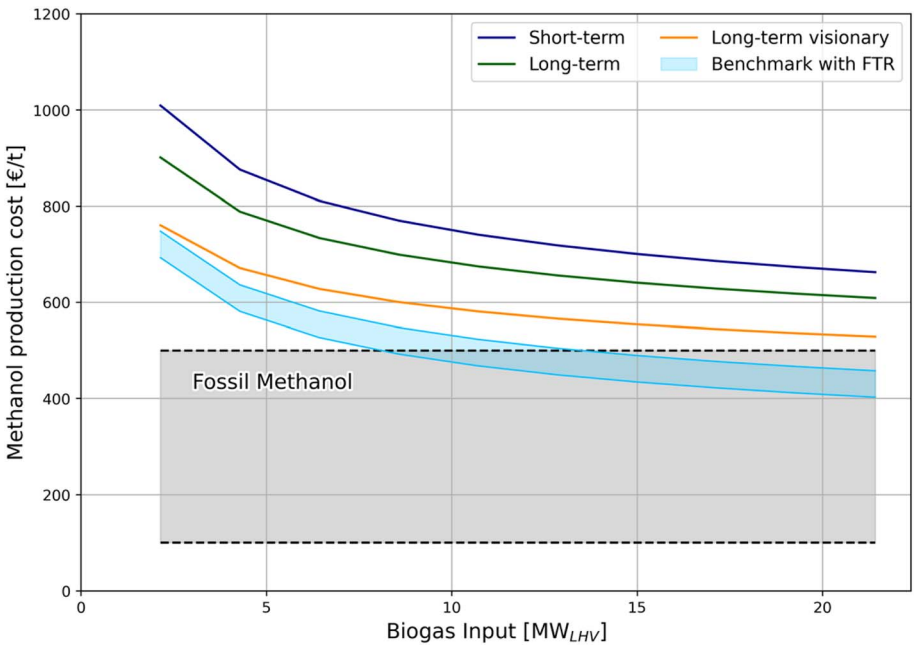

Fig. 12 Impact of economies of scale on methanol production cost in different economic scenarios and comparison with fossil methanol and bio-methanol with an FTR-based plant (benchmark). Shaded area for the benchmark considering electricity prices of 50–150 € MWh^{-1}.

The increased methanol production at a higher methanol selling price involves a reduction of the impact of the methane slip, as these fixed upstream emissions are distributed over a larger amount of methanol. Overall, specific emissions remain rather stable, as the benefit of the augmented methanol yield is offset by the additional embodied emissions associated with the expanded renewable capacity. Overall, the total specific emissions are between 5 $g_{CO_2,eq}/MJ_{LHV}$ (low emission scenario) and 18 $g_{CO_2,eq}/MJ_{LHV}$ (high emission scenario). For comparison, the bio-methanol production *via* FTR results in specific emissions related to biomethane slip ranging between 3 and 13 $g_{CO_2,eq}/MJ_{LHV}$ and a total emission of circa 3.6–14.2 $g_{CO_2,eq}/MJ_{LHV}$.

Methanol production from natural gas with end-of-life combustion entails emissions of about 110 $g_{CO_2,eq}/MJ_{LHV}$.[62] This value comprises supply chain emissions (gas production and transport, intermediate processing and transport, production and methanol transport) of roughly 40 $g_{CO_2,eq}/MJ_{LHV}$ and end-of-life emissions equal to 69 $g_{CO_2,eq}/MJ_{LHV}$. In contrast to production from natural gas, when methanol is produced from biogenic carbon, end-use emissions are considered climate neutral.[62] While the specific emissions of the eSMR process (evaluated as $g_{CO_2,eq}/MJ_{LHV}$ of methanol) are slightly higher than those of the FTR configuration, evaluating the emission reduction against fossil methanol per unit of consumed biogas

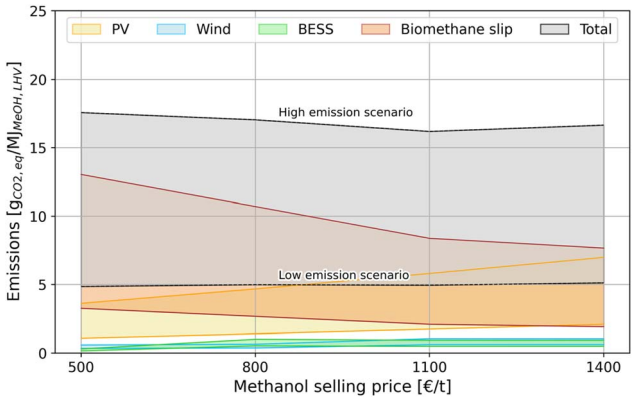

Fig. 13 Emissions associated with power production (REN & BESS) and biogas production (methane slip). Each shaded area is bounded by the results of the low- and high-emission scenarios. The plot is produced for the "flexible" case in South Italy, under long-term economic assumptions.

reveals a different perspective. Due to its higher carbon efficiency, the emission reduction achieved by the bio-e-methanol pathway can be significantly greater, ranging from approximately 70 to 140 $g_{CO_2,eq}/MJ_{biogas}$. In contrast, the avoided emissions for the FTR case are limited to between 77 and 86 $g_{CO_2,eq}/MJ_{biogas}$. Therefore, bio-e-methanol yields higher overall emission reductions when the system operates at high carbon efficiency (*e.g.*, by restricting ICE usage and integrating hydrogen into the process). In comparison, when substituting fossil natural gas with bio-methane, the avoided emissions are lower, amounting to approximately 58–64 $g_{CO_2,eq}/MJ_{biogas}$. This calculation is based on natural gas emission data from ref. 63, assuming methane leakage rates between 0.2% and 3.5%.

4 Conclusions

This study presented a comprehensive techno-economic optimisation of a flexible bio-e-methanol plant, integrating biogas reforming *via* electrified Steam Methane Reforming (eSMR) and external electrolytic hydrogen. The eSMR process demonstrates superior resource utilisation compared to conventional fired tubular reforming (FTR), boosting carbon efficiency from ~50% to 70% in the base load configuration and up to 96% in the enhanced MeOH mode *via* hydrogen injection. However, higher carbon recovery involves higher electricity consumption, reaching 3.25 kWh/kg_{MeOH} at base load and 5.46 kWh/kg_{MeOH} in enhanced methanol mode (*i.e.* when methanol yield is boosted by the addition of hydrogen from water electrolysis), compared to 0.55 kWh/kg_{MeOH} for a conventional FTR-based plant.

The system was integrated with renewable solar and wind power generation with a BESS, a biogas Internal Combustion Engine for power self-generation during periods of low renewable availability, and intermediate gas/liquid buffers to unlock the operational flexibility of the chemical island. The system was optimised with hourly resolution over a full year, evaluating: (i) different degrees of flexibility; (ii) two distinct European locations; (iii) the sensitivity to methanol selling price; (iv) various economic scenarios regarding the costs of renewable technologies, batteries, and electrolysers; and (v) the impact of economies of scale (from 390 $Nm^3\ h^{-1}$ to 3900 $Nm^3\ h^{-1}$ of biogas).

The analysis demonstrates that the flexibility of syngas generation and methanol synthesis, combined with biogas and methanol storage, enables the capture of the majority of the load-following economic benefits. This strategy effectively reduces electricity curtailment and lowers the specific methanol production cost by up to 24%. However, the advantages associated with flexibility diminish in the long term scenario as a result of the decreasing costs of renewable technologies and batteries. Moving to an "enhanced flexibility" configuration, including hydrogen and syngas storage and load decoupling between syngas generation and methanol synthesis units, yields only marginal improvements, increasing the NPV by only 2–7% and the internal rate of return by less than 1 percentage point. Across the analysed frameworks, the flexible plant achieves profitability at methanol selling prices between 600 and 800 € t^{-1}, with IRR values reaching up to 15–30% at a methanol selling price of 1100 € t^{-1}.

The eSMR process entails lower specific plant costs compared to the conventional FTR-based process, thanks to the higher compactness of the reformer and to the higher methanol production capacity. Ultimately, the competitiveness between the two technologies is largely influenced by the relative cost of biogas compared to electricity: if biogas is cheaper than electricity, burning part of the feedstock to fire the FTR furnace is economically more competitive than electrifying the reformer in most scenarios. Nevertheless, the increased methanol yield of the eSMR process allows it to become economically viable at high methanol selling prices. In this study, given the higher cost of electricity compared to biogas, the augmented production of the eSMR configuration makes the process competitive (yielding a higher NPV) for methanol prices exceeding 1100 € t^{-1} in the short-term scenario and for values greater than 550–800 € t^{-1} in the long-term scenarios.

Installing an electrolyser remains economically challenging: under standard cost projections, hydrogen addition only becomes viable at methanol prices exceeding 1000 € t^{-1}, whereas a "long-term visionary" reduction in electrolyser CAPEX (363 € kW^{-1}) is required to unlock its potential at lower market prices.

The inherent complexity and capital intensity of this integrated process suggest that it is best suited for large-scale applications. Transitioning from small, distributed plants to large, centralised plants collecting biogas from multiple sources leverages significant economies of scale, driving the specific methanol production cost down from 760–1009 € t^{-1} for 390 $Nm^3\ h^{-1}$ (2.1 MW_{LHV}) plants to 529–663 € t^{-1} for 3900 $Nm^3\ h^{-1}$ (21 MW_{LHV}) plants. Furthermore, environmental analysis highlights that while the specific emissions per unit of methanol are slightly higher for the eSMR process when accounting for the embedded emissions of REN/BESS, the eSMR pathway offers a greater reduction in avoided CO_2 emissions per unit of utilised biogas. Provided that the system's carbon efficiency is effectively maximised, the eSMR configuration can reach up to 140 $g_{CO_2,eq}/MJ_{biogas}$ of avoided emissions, compared to approximately 80 $g_{CO_2,eq}/MJ_{biogas}$ for bio-methanol from the FTR-based process and

60 $g_{CO_2,eq}/MJ_{biogas}$ for the substitution of fossil methane with biomethane.

Author contributions

Andrea Nava: writing – original draft, visualisation, software, methodology, investigation, formal analysis, and conceptualisation. Matteo C. Romano: writing – review and editing, validation, supervision, methodology, and conceptualisation.

Conflicts of interest

There are no conflicts of interest to declare.

Abbreviations

BCM	Billion cubic metres
BCY	Battery equivalent cycle number
BESS	Battery energy storage system
CAPEX	CAPital EXpenditure
CF	Capacity factor
CRF	Capital recovery factor
eSMR	Electrified steam methane reformer
EE	Electric energy
FTR	Fired tubular reformer
GHSV	Gas hourly space velocity
ICE	Internal combustion engine
IRR	Internal rate of return
KPIs	Key performance indicators
LCOE	Levelised cost of electricity
LCOM	Levelised cost of methanol
LHV	Lower heating value
M	Stoichiometric module of the syngas
MILP	Mixed integer linear programming
Mt	Million tonnes
NPV	Net present value
OPEX	OPerative EXpenditure
PI	Profitability index
REN	Renewable energy
SMR	Steam methane reforming
SoC	State of charge
STH	Storage hours
TAC	Total annual cost

Data availability

The data supporting the findings of this study, including all assumptions, methodologies used to simulate the plants on Aspen and GAMS, and all results, are provided in the main paper and the supplementary information (SI). Supplementary information: detailed process flow diagrams and comprehensive stream tables detailing properties and compositions across different operating points; methanol reactor performance data, including its response to varying recycle ratios with and without hydrogen addition, alongside specific equipment cost estimations; the complete mathematical formulation of the optimisation model, including all governing equations and constraints; granular cost breakdowns and specific capital expenditure estimations for all chemical island components; and comprehensive tables detailing the optimisation results, including renewable and storage unit capacities, the Levelised Cost of Energy (LCOEren), capacity factors, and key economic indices across all evaluated scenarios and varying methanol selling prices. See DOI: https://doi.org/10.1039/d6se00355a.

References

1 IEA, *Outlook for Biogas and Biomethane*, IEA, Paris, 2025, https://www.iea.org/reports/outlook-for-biogas-and-biomethane, Licence: CC BY 4.0. n.d.

2 EBA, *European Biogas Association Statistical Report 2024*, Brussels, Belgium, 2024, December 2024. n.d.

3 L. Zheng, M. Ambrosetti and E. Tronconi, Joule-Heated Catalytic Reactors toward Decarbonization and Process Intensification: A Review, *ACS Eng. Au*, 2024, **4**, 4–21, DOI: 10.1021/acsengineeringau.3c00045.

4 D. Spagnolo, L. Cornett and K. Chuang, Direct electro-steam reforming: a novel catalytic approach, *Int. J. Hydrogen Energy*, 1992, **17**, 839–846, DOI: 10.1016/0360-3199(92)90033-S.

5 M. N. Pérez-Camacho, J. Abu-Dahrieh, D. Rooney and K. Sun, Biogas reforming using renewable wind energy and induction heating, *Catal. Today*, 2015, **242**, 129–138, DOI: 10.1016/j.cattod.2014.06.010.

6 S. T. Wismann, J. S. Engbæk, S. B. Vendelbo, F. B. Bendixen, W. L. Eriksen, K. Aasberg-Petersen, *et al.*, Electrified methane reforming: A compact approach to greener industrial hydrogen production, *Science*, 2019, **364**, 756–759, DOI: 10.1126/SCIENCE.AAW8775/SUPPL_FILE/AAW8775-WISMANN-SM.PDF.

7 S. T. Wismann, J. S. Engbæk, S. B. Vendelbo, W. L. Eriksen, C. Frandsen, P. M. Mortensen, *et al.*, Electrified Methane Reforming: Understanding the Dynamic Interplay, *Ind. Eng. Chem. Res.*, 2019, **58**, 23380–23388, DOI: 10.1021/acs.iecr.9b04182.

8 S. T. Wismann, J. S. Engbæk, S. B. Vendelbo, W. L. Eriksen, C. Frandsen, P. M. Mortensen, *et al.*, Electrified methane reforming: Elucidating transient phenomena, *Chem. Eng. J.*, 2021, **425**, 131509, DOI: 10.1016/J.CEJ.2021.131509.

9 Topsoe, eREACT™ Hydrogen: The future of blue hydrogen|Equipment|Products|Topsoe n.d., https://www.topsoe.com/our-resources/knowledge/our-products/equipment/ereact-hydrogen.

10 T. N. From, B. Partoon, M. Rautenbach, M. Østberg, A. Bentien, K. Aasberg-Petersen, *et al.*, Electrified steam methane reforming of biogas for sustainable syngas manufacturing and next-generation of plant design: A pilot plant study, *Chem. Eng. J.*, 2024, **479**, 147205, DOI: 10.1016/J.CEJ.2023.147205.

11 T. N. From, M. Rautenbach, B. Partoon, M. Østberg, S. T. Wismann, A. Bentien, *et al.*, Understanding the dynamic interplay of CH4/CO2 ratio in electrified reforming of biogas to renewable methanol production: A

pilot plant story, *Chem. Eng. J.*, 2025, **518**, 164662, DOI: 10.1016/J.CEJ.2025.164662.
12 T. N. From, M. Lobban, V. B. Terkelsen, J. Visagie, B. Partoon, S. T. Wismann, *et al.*, Interchangeable biogas and CO2 valorization through electrified syngas manufacturing for synthetic fuel production, *J. CO2 Util.*, 2026, **105**, 103331, DOI: 10.1016/j.jcou.2026.103331.
13 E. Meloni, M. Martino, A. Ricca and V. Palma, Ultracompact methane steam reforming reactor based on microwaves susceptible structured catalysts for distributed hydrogen production, *Int. J. Hydrogen Energy*, 2021, **46**, 13729–13747, DOI: 10.1016/j.ijhydene.2020.06.299.
14 R. Balzarotti, M. Ambrosetti, A. Beretta, G. Groppi and E. Tronconi, Investigation of packed conductive foams as a novel reactor configuration for methane steam reforming, *Chem. Eng. J.*, 2020, **391**, 123494, DOI: 10.1016/j.cej.2019.123494.
15 M. Ambrosetti, D. Bonincontro, R. Balzarotti, A. Beretta, G. Groppi and E. Tronconi, H2 production by methane steam reforming over Rh/Al2O3 catalyst packed in Cu foams: A strategy for the kinetic investigation in concentrated conditions, *Catal. Today*, 2022, **387**, 107–118, DOI: 10.1016/j.cattod.2021.06.003.
16 R. Balzarotti, A. Beretta, G. Groppi and E. Tronconi, A comparison between washcoated and packed copper foams for the intensification of methane steam reforming, *React. Chem. Eng.*, 2019, **4**, 1387–1392, DOI: 10.1039/C9RE00125E.
17 L. Zheng, M. Ambrosetti, F. Zaio, A. Beretta, G. Groppi and E. Tronconi, Direct electrification of Rh/Al2O3 washcoated SiSiC foams for methane steam reforming: An experimental and modelling study, *Int. J. Hydrogen Energy*, 2023, **48**, 14681–14696, DOI: 10.1016/J.IJHYDENE.2022.12.346.
18 L. Zheng, M. Ambrosetti, D. Marangoni, A. Beretta, G. Groppi and E. Tronconi, Electrified methane steam reforming on a washcoated SiSiC foam for low-carbon hydrogen production, *AIChE J.*, 2023, **69**, e17620, DOI: 10.1002/AIC.17620;WGROUP:STRING:PUBLICATION.
19 G. Ferri, M. Ambrosetti, A. Beretta, G. Groppi and E. Tronconi, Experimental investigation and 2D mathematical modelling of copper foams packed with Rh-Al2O3 catalysts for the intensification of methane steam reforming, *Catal. Today*, 2024, **426**, 114386, DOI: 10.1016/J.CATTOD.2023.114386.
20 G. Ferri, M. Ambrosetti, A. Beretta, G. Groppi, E. Tronconi and A. Agosti, A novel electrified methane steam reformer for intensified H2 production based on conductive packed foams: experimental and modelling assessment, *Chem. Eng. J.*, 2025, **523**, 168753, DOI: 10.1016/J.CEJ.2025.168753.
21 T. Laird, Ullmann's Encyclopedia of Industrial Chemistry, 5th Edition VCH: Weinheim, Germany. 1996/1997. Section A, 28 vols Section B, 8 vols DM 19 400, *Org. Process Res. Dev.*, 1997, **1**, 391–392, DOI: 10.1021/op970020u.
22 V. D. Phillips, C. M. Kinoshita, D. R. Neill and P. K. Takahashi, Thermochemical production of methanol from biomass in Hawaii, *Appl. Energy*, 1990, **35**, 167–175, DOI: 10.1016/0306-2619(90)90066-M.
23 L. R. Clausen, N. Houbak and B. Elmegaard, Technoeconomic analysis of a methanol plant based on gasification of biomass and electrolysis of water, *Energy*, 2010, **35**, 2338–2347, DOI: 10.1016/j.energy.2010.02.034.
24 R. Rinaldi, G. Lombardelli, M. Gatti, C. G. Visconti and M. C. Romano, Techno-economic analysis of a biogas-to-methanol process: Study of different process configurations and conditions, *J. Clean. Prod.*, 2023, **393**, 136259, DOI: 10.1016/J.JCLEPRO.2023.136259.
25 A. Poluzzi, G. Guandalini, S. Guffanti, M. Martinelli, S. Moioli, P. Huttenhuis, *et al.*, Flexible Power and Biomass-To-Methanol Plants With Different Gasification Technologies, *Front. Energy Res.*, 2022, **9**, 795673, DOI: 10.3389/FENRG.2021.795673/BIBTEX.
26 A. Poluzzi, G. Guandalini, F. d'Amore and M. C. Romano, The Potential of Power and Biomass-to-X Systems in the Decarbonization Challenge: a Critical Review, *Curr. Sustain. Renew. Energy Rep.*, 2021, **8**, 242–252, DOI: 10.1007/S40518-021-00191-7/FIGURES/2.
27 G. Bozzano, C. Pirola, C. Italiano, R. Pelosato, A. Vita and F. Manenti, *Biogas: a Possible New Pathway to Methanol?*, 2017, pp. 523–528, DOI: 10.1016/B978-0-444-63965-3.50089-1.
28 A. Vita, C. Italiano, D. Previtali, C. Fabiano, A. Palella, F. Freni, *et al.*, Methanol synthesis from biogas: A thermodynamic analysis, *Renew. Energy*, 2018, **118**, 673–684, DOI: 10.1016/j.renene.2017.11.029.
29 R. O. dos Santos, L. D. S. Santos and D. M. Prata, Simulation and optimization of a methanol synthesis process from different biogas sources, *J. Clean. Prod.*, 2018, **186**, 821–830, DOI: 10.1016/j.jclepro.2018.03.108.
30 S. Ghosh, V. Uday, A. Giri and S. Srinivas, Biogas to methanol: A comparison of conversion processes involving direct carbon dioxide hydrogenation and *via* reverse water gas shift reaction, *J. Clean. Prod.*, 2019, **217**, 615–626, DOI: 10.1016/j.jclepro.2019.01.171.
31 B. Hernández and M. Martín, Optimal Process Operation for Biogas Reforming to Methanol: Effects of Dry Reforming and Biogas Composition, *Ind. Eng. Chem. Res.*, 2016, **55**, 6677–6685, DOI: 10.1021/acs.iecr.6b01044.
32 J. P. Sheets and A. Shah, Techno-economic comparison of biogas cleaning for grid injection, compressed natural gas, and biogas-to-methanol conversion technologies, *Biofuel Bioprod. Biorefining*, 2018, **12**, 412–425, DOI: 10.1002/bbb.1848.
33 L. Salano, M. M. Bozzini, E. Moioli and F. Manenti, Comparative techno-economic analysis on a biogas reforming plant: Case study on partial upgrading with a pressure swing water absorption, *Chem. Eng. Sci.*, 2026, **321**, 122602, DOI: 10.1016/j.ces.2025.122602.
34 C. Dannesboe, J. B. Hansen and I. Johannsen, Removal of sulfur contaminants from biogas to enable direct catalytic methanation, *Biomass Convers. Biorefin.*, 2021, **11**, 1823–1834, DOI: 10.1007/s13399-019-00570-7.
35 K. M. Vanden Bussche and G. F. Froment, A Steady-State Kinetic Model for Methanol Synthesis and the Water Gas

Shift Reaction on a Commercial Cu/ZnO/Al2O3Catalyst, *J. Catal.*, 1996, **161**, 1–10, DOI: 10.1006/JCAT.1996.0156.
36 A. Nava, D. Remondini, S. Campanari and M. C. Romano, Carbon-negative "emerald hydrogen" from electrified steam methane reforming of biogas: System integration and optimization, *Int. J. Hydrogen Energy*, 2024, **88**, 1237–1255, DOI: 10.1016/J.IJHYDENE.2024.09.171.
37 R. Turton, R. C. Bailie, W. B. Whiting and J. A. Shaeiwitz, *Analysis, Synthesis, and Design of Chemical Processes*, Prentice Hall, 2012.
38 L. Riva, I. Martínez, M. Martini, F. Gallucci, M. van Sint Annaland and M. C. Romano, Techno-economic analysis of the Ca-Cu process integrated in hydrogen plants with CO2 capture, *Int. J. Hydrogen Energy*, 2018, **43**, 15720–15738, DOI: 10.1016/j.ijhydene.2018.07.002.
39 The Chemical Engineering Plant Cost Index®, *Chemical Engineering*, n.d. https://www.chemengonline.com/pci-home.
40 IRENA, *Renewable Power Generation Costs in 2024*, International Renewable Energy Agency, Abu Dhabi, 2025.
41 Data|Electricity, ATB, NREL, 2023, n.d. https://atb.nrel.gov/electricity/2023/data, accessed November 27, 2023.
42 U.S. Department of Energy (DOE), *Pathways to Commercial Liftoff: Clean Hydrogen, Update 2024*, Washington, D.C., December 2024. n.d.
43 Hydrogen Council and McKinsey & Company, *Hydrogen Insights 2023: the State of the Global Hydrogen Economy, with a Deep Dive into Renewable Hydrogen Cost Evolution*, Hydrogen Council, December 2023. n.d.
44 IRENA, *Making the breakthrough: green hydrogen policies and technology costs*, 2021, https://www.irena.org/-/media/Files/IRENA/Agency/Publication/2020/Nov/IRENA_Green_Hydrogen_breakthrough_2021.pdf.
45 M. Ram, T. Galimova, D. Bogdanov, M. Fasihi, A. Gulagi and C. Breyer, *et al.*, *POWERFUELS in a Renewable Energy World*, 2020.
46 S. Pfenninger and I. Staffell, Long-term patterns of European PV output using 30 years of validated hourly reanalysis and satellite data, *Energy*, 2016, **114**, 1251–1265, DOI: 10.1016/j.energy.2016.08.060.
47 A. Müller, L. Friedrich, C. Reichel, S. Herceg, M. Mittag and D. H. Neuhaus, A comparative life cycle assessment of silicon PV modules: Impact of module design, manufacturing location and inventory, *Sol. Energy Mater. Sol. Cells*, 2021, **230**, 111277, DOI: 10.1016/J.SOLMAT.2021.111277.
48 M. Kolahchian Tabrizi, J. Famiglietti, D. Bonalumi and S. Campanari, The Carbon Footprint of Hydrogen Produced with State-of-the-Art Photovoltaic Electricity Using Life-Cycle Assessment Methodology, *Energies*, 2023, **16**, 5190, DOI: 10.3390/EN16135190/S1.
49 A. Schreiber, J. Marx and P. Zapp, Comparative life cycle assessment of electricity generation by different wind turbine types, *J. Clean. Prod.*, 2019, **233**, 561–572, DOI: 10.1016/J.JCLEPRO.2019.06.058.
50 D. Bonalumi and T. M. Kolahchian, Re-evaluation of the Global Warming Potential for the Production of Lithium-Ion Batteries with Nickel-Manganese-Cobalt Cathode Chemistries in China, *Energy Fuels*, 2022, **36**, 13753–13767, DOI: 10.1021/ACS.ENERGYFUELS.2C02204/ASSET/IMAGES/MEDIUM/EF2C02204_0013.GIF.
51 IEA Bioenergy Task 37, *Methane Emissions from Biogas Plants Methods for Measurement, Results and Effect on Greenhouse Gas Balance of Electricity Produced*, 2017.
52 O. Hurtig, M. Buffi, R. Besseau, N. Scarlat, C. Carbone and A. Agostini, Mitigating biomethane losses in European biogas plants: A techno-economic assessment, *Renew. Sustain. Energy Rev.*, 2025, **210**, 115187, DOI: 10.1016/J.RSER.2024.115187.
53 NREL (National Renewable Energy Laboratory), *2024 Annual Technology Baseline*, Golden, CO, National Renewable Energy Laboratory, 2024, https://atb.nrel.gov/. n.d.
54 W. Cole, A. W. Frazier and C. Augustine, *Cost Projections for Utility-Scale Battery Storage : 2021 Update*, National Renewable Energy Laboratory, 2020, NREL/TP-6A20-79236.
55 ASUE and Stadt Frankfurt am Main, *BHKW-kenndaten*, 2011. n.d.
56 U.S. Department of Energy (DOE), Fuel Cell Technologies Office Multi-Year Research, Development, and Demonstration Plan - Section 3.3 Hydrogen Storage, 2015.
57 J. Apt, A. Newcomer, L. B. Lave, S. Douglas and L. M. Dunn, *An Engineering-Economic Analysis of Syngas Storage*, US Department of Energy's National Energy Technology Laboratory, 2008, p. 143.
58 G. Herz, E. Reichelt and M. Jahn, Design and evaluation of a Fischer-Tropsch process for the production of waxes from biogas, *Energy*, 2017, **132**, 370–381, DOI: 10.1016/j.energy.2017.05.102.
59 Biomethane Industrial Partnership, *Insights into the Current Costs of Biomethane Production from Real Industry Data*, October 2023, Prepared by Task Force 4.2. n.d.
60 IEA, *Sustainable supply potential and costs – Outlook for biogas and biomethane: Prospects for organic growth – Analysis*, IEA, 2020, https://www.iea.org/reports/outlook-for-biogas-and-biomethane-prospects-for-organic-growth/sustainable-supply-potential-and-costs.
61 IRENA and Methanol Institute, *Innovation Outlook : Renewable Methanol*, International Renewable Energy Agency, Abu Dhabi, 2021.
62 C. Hamelinck and M. Bunse, Carbon footprint of methanol For: Methanol Institute n.d. https://methanol.org/wp-content/uploads/2022/01/Carbon-Footprint-of-Methanol-studio-Gear-Up-Full-Presentation.pdf.
63 M. C. Romano, C. Antonini, A. Bardow, V. Bertsch, N. P. Brandon, J. Brouwer, *et al.*, Comment on "How green is blue hydrogen?, *Energy Sci. Eng.*, 2022, **10**, 1944–1954, DOI: 10.1002/ese3.1126.